# Design of a Test Rig for Conductive Ball Bearing Greases

A Major Qualifying Project Report
Submitted to the Faculty
of
WORCESTER POLYTECHNIC INSTITUTE
in Partial Fulfillment of the Requirements for the
Degree of Bachelor of Science by:


Samantha E. Robinson

With co-authors at Kungliga Tekniska Högskolan:

Gabriel Benjamin Calderon Salmeron

Siddharth Ramakrishnan

Vignesh Nagarajan

Nikhil Marharshi

Ruben Noya


Professor Holly K. Ault, Advisor

Submitted on May 19, 2018


This report represents the work of a WPI undergraduate student. It has been submitted to the faculty as evidence of completion of a degree requirement. WPI publishes these reports on its website without editorial or peer review.

# ABSTRACT

Modern electric machinery requires the use of conductive ball bearing greases. The project sponsor, Axel Christiernsson International AB, has outlined requirements for a device to test grease under simulated conditions of an electric motor. The machine combines all of the requirements, including operating at speeds above 10,000rpm, measuring milli-Newton-meter range torques, and isolating an electric current to the test bearing. This report outlines the process to design a test rig to be constructed in August 2018. The final design consists of a belt transmission, ceramic support bearings, cantilevered test bearing in custom housing, an electric circuit, nut and screw loading, PT100 temperature sensor, and friction torque measurement by load cells.

# ACNOWLEDGMENTS

This project would not be possible without the help from many different individuals. First, I would like to thank Worcester Polytechnic Institute (WPI) and the Interdisciplinary and Global Studies Division for allowing me the opportunity to complete this project in Stockholm, Sweden. I have the deepest gratitude for my advisor, Professor Holly Ault, for making this project possible and advising me during the project.

I would like to thank the Royal Institute of Technology (KTH) and their Machine Design department for allowing me to partake in the project in the MF2076 VT18-1 Machine Design Advanced Course Part 1. I would particularly like to thank the course professors Kjell Andersson and Stefan Björklund for advising my team and I throughout the project. Thanks to Sergei Glavatskih and Akepati Bhaskar Reddy for technical advice during the design process. I would also like to thank Lasse Wingård for coordinating between WPI and KTH and for making me feel comfortable and welcome in Stockholm.

Finally, thanks to my team members during this project. Thank you Gabriel Benjamin Calderon Salmeron, Siddharth Ramakrishnan, Vignesh Nagarajan, Nikhil Marharshi, and Ruben Noya for not only working by my side to complete this project, but also for becoming my friends along the way. An additional thank you to my fellow WPI student, Olivia Steen, for reaching out to me about this opportunity, traveling with me to Sweden, and becoming an amazing friend.

# TABLE OF CONTENTS

1 INTRODUCTION ..... 7

1.1 Customer Profile ..... 8

1.2 Problem Definition ..... 9

1.3 Project Scope ..... 10

1.3.1 Mandatory Requirements ..... 10

1.3.2 Desired Requirements ..... 10

1.3.3 Design Challenges ..... 10

1.4 Report Outline ..... 14

2 BACKGROUND ..... 15

2.1 Existing Test Rigs ..... 15

2.1.1 Start-Stop Journal Bearing Test Rig ..... 15

2.1.2 Skf Rof+ Test Rig ..... 16

2.1.3 Bearing Electro Corrosion Tester ..... 17

2.1.4 Deep Groove Ball Bearing Test Rig ..... 17

2.2 Friction Torque ..... 18

2.2.1 Torque Estimation ..... 18

2.2.2 Direct Torque Measurement ..... 22

2.2.3 Indirect Friction Torque Measurement ..... 25

2.3 Loading Mechanisms ..... 27

2.3.1 Actuators ..... 28

2.3.2 Nut and Screw ..... 29

2.4 High Speed Transmission System ..... 29

2.4.1 Belt Transmission System ..... 30

2.4.2 High Speed Motors-Shaft Coupling ..... 31
2.5 Temperature Measurement ..... 33
2.6 Electric Potential ..... 34
2.6.1 Power Supply ..... 34
2.6.2 Signal Generator ..... 35
2.6.3 Isolation Of Current ..... 35
2.6.4 Voltage Controlled Resistor (Vcr) ..... 36
2.6.5 Electric Circuit ..... 36
2.7 Bearing Seals ..... 37
2.7.1 Antifriction Contact Seals ..... 37
2.7.2 Centritec Non-Contact Seals ..... 38

3 DESIGNS ..... 39
3.1 Initial Concepts ..... 39
3.2 Refined Concepts ..... 40
3.2.1 Design A: Cantilever Concept ..... 40
3.2.2 Design B: Central Loading ..... 42
3.2.3 Design C: Two Test Bearings ..... 43
3.2.4 Design D: Four Test Bearings ..... 44
3.2.5 Design E: Advanced Cantilever ..... 45
3.3 Design Evaluation ..... 46
3.3.1 Morphological Chart ..... 46
3.3.2 Pugh's Matrix ..... 47

4 ANALYSIS ..... 49
4.1 Static Analysis ..... 49
4.1.1 Forces ..... 49
4.1.2 Static Stresses, Slope, And Deflection ..... 50
4.2 Dynamic Analysis ..... 50
4.2.1 Critical Speed ..... 51

5 CONCLUSION ..... 52
6 RECOMMENDATIONS AND FUTURE WORK ..... 53

7 REFERENCES ..... 54
8 APPENDIX ..... 55
8.1 Appendix A: MATLAB Code for Angular Twist ..... 55
8.2 Appendix B: Original Stepped Shaft MATLAB by Stefan Bjorklund 62
8.3 Appendix C: Design Component Comparison ..... 70

# 1 INTRODUCTION

As popularity in environmental issues increases, the demand for sustainable systems also has been increasing in the past few decades. These systems include electric machinery, such as electric cars, to minimize the effects of fossil fuels. The recent demand has driven developments in technology to be more energy efficient by relying on complex electric systems. As this technology improves, the efficiency of these sustainable alternatives is also improving.

One aspect of technology that must progress is ball bearings because of the rotating components in the electric mechanisms. For example, the conditions of the bearings in electrical applications of hybrid or electric cars are different than those of regular cars. The main difference is the electrical potential generated by electric components. These components include variable frequency drives (VFD) and alternators, which induce stray currents into the rotating shaft. This is an issue for the lifetime of bearings because they typically act as the least path of resistance for these currents. To lessen this impact, non-conductive greases are applied to both reduce friction and act as insulator. Once sufficient charge gets accumulated in the inner ring of the bearing, it breaks the insulation and an electric discharge takes place causing micro welding. This discharge has negative influence on bearing performance and can lead to premature bearing failure.

Several methods such as full ceramic ball bearings have been used for avoiding this kind of problem; however, they are very expensive and cannot be considered in mass production systems as in the automotive industry. For this reason, new less expensive methods are being developed. One solution is the development of new conductive greases that do not accumulate charge during the machine operation.

This project covers the design a device to simulate the electrical and mechanical conditions on bearings in electrical machinery. Grease in deep grove ball bearings will be tested in the mechanism as friction is measured. The results will assist in performance evaluation and improvement of conductive greases by Axel Christiernsson International AB.

## 1.1 Customer Profile

The sponsor and customer of this project is Axel Christiernsson International AB, a lubricating grease company based in Sweden. The Table 1 shows the profile of this company and some of its characteristics.

**Table 1. Customer Profile**

| | | |
|---|---|---|
| Company Name | Axel Christiernsson International AB | |
| Project responsible and email | Johan Leckner – johan.leckner@axel.com | |
| Logo | AXEL<br>AXEL CHRISTIERNSSON | |
| Website | http://www.axelch.com/ | |
| Founded | 1888 | |
| Headquarters Location and Production Capacity (Tonnes) | Nol, Sweden<br>(North of Gothenburg). | 12000 |
| Branches location and Production Capacity (Tonnes) | Netherlands<br>France<br>USA | 17000 |
| Main Business Focus | Production of lubricating greases | |
| Other Services | ● Training<br>● Application evaluation and troubleshooting analysis<br>● Product development<br>● Marketing and sales training (greases)<br>● Logistics and inventory of greases training | |
| Customer Industries | ● Automobile and transportation<br>● Mining<br>● Food and beverage<br>● Steel mills<br>● Marine<br>● Agriculture and forestry<br>● Pulp and paper<br>● Power generation and steel mills | |

From this table, this project is concerned with the product development of lubricating greases for automobile and transportation purposes. In addition to the information in the customer profile, the business strategy of the company is necessary to understand their

process. Axel Christiernsson International AB has a Customised Label™ strategy that is pictured below.

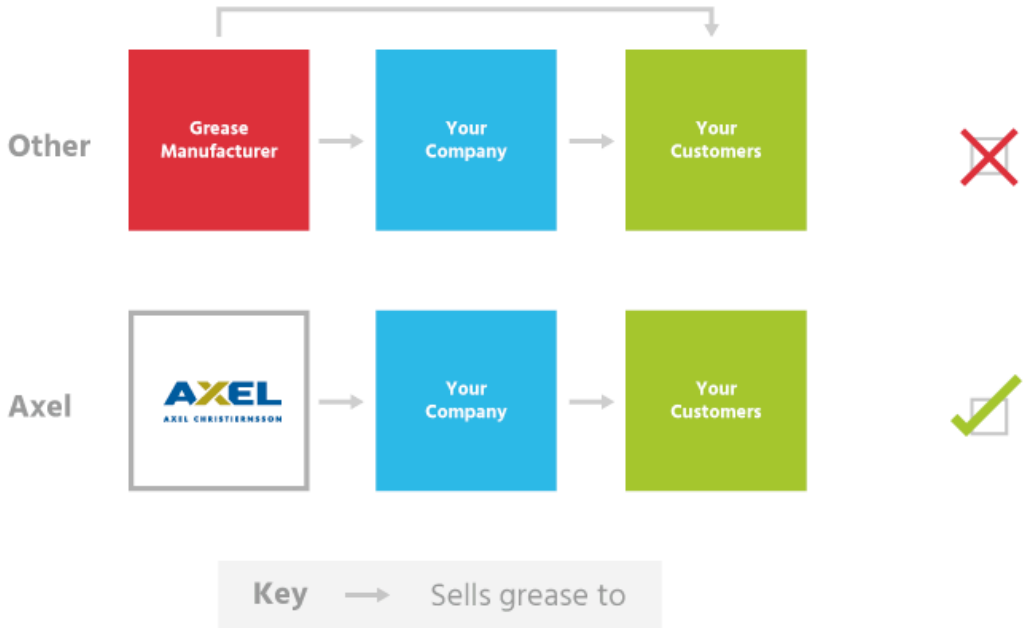


**Figure 1. Company Strategy (Axel Christiernsson, 2018)**

The lubricants produced by Axel Christiernsson are not directly sold with their brand to consumers. Their customers are intermediate companies that put their name on the product and sell the product under its brand.

## 1.2 Problem Definition

Axel Christiernsson needs a device to test the conditions of their greases for electrical machinery applications. This test rig is critical to the company in order to understand the practical abilities of their new products, to develop information to display to their customers, and to improve the products for the long-term success of the organization. The problem stems from the lack of a machine of this nature, especially with the exact conditions that the company desires. These conditions include a specific type of bearings and various lubricant combinations, as well as the input velocities and loads. The main outputs of the testing device should be the temperatures and friction torque of bearings. The company has outlined the specific conditions in the following section.

## 1.3 Project Scope

The goal of this project is to evaluate conductive grease in deep groove ball bearings under conditions that simulate those in an electric motor. The project requirements are based on the customer specification and they are divided in two different groups: the mandatory and desired. The mandatory requirements are non-negotiable conditions that must be fulfilled, and the desired are the requirements that will add additional value to the final test rig.

### 1.3.1 Mandatory Requirements

- Test deep groove ball bearing (620X) with various greases
- Apply an electric potential across the bearing from 1 to 2 volts
- Achieve speed factors from 600,000 to 800,000 NDm
- Measure torque caused by the friction of the test bearing
- Change the loads on the bearing in the range of 50 to 1000 N
- Log the self-induced temperature during the test

### 1.3.2 Desired Requirements

- Avoid additional friction, such as by contact seals
- Vary the speed of the shaft
- Remove and replace the test bearing quickly and easily
- Test multiple bearing sizes with the same mechanism
- Increase stability and safety by minimizing misalignment
- Increase life of the test rig itself, such as the motor, support bearings, etc.

### 1.3.3 Design Challenges

Based on the user requirements and from the design point of view, the project has several challenges or risks that should be considered from the design phase. These risks are

mainly related to the operation at high speeds, measurement of friction torque, and application of the electrical potential.

Shaft Speeds

One of the user requirements states that the speed of the shaft should be between 600.000 and 800.000NDm. NDm is the method of calculation of speed factor that defines the relation of the speed at which the bearing rotates with the size of the bearing. This value is calculated by using the bearing's median size or pitch diameter, and the rotation speed (Noria Corporation, n.d.). The formula that defines the speed factor is shown below.

$$Speed\ factor = N * Dm = N * \frac{Do - Di}{2}$$

*Equation 1:* $Speed\ factor = N * Dm = N * \frac{Do - Di}{2}$

Where Speed factor is in [mm/min]

N: Bearing speed [min-1]

Dm: Bearing pitch diameter [mm]

Do: Bearing outer diameter

Di: Bearing inner diameter

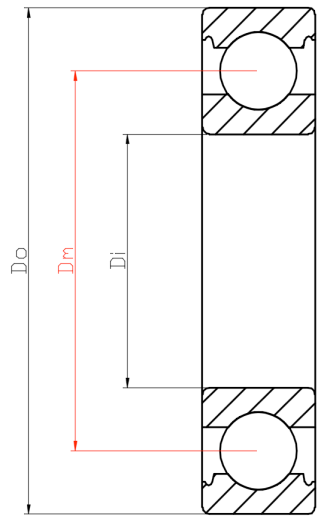


**Figure 2. Deep Groove Ball Bearing**

Based on the required speed factor, the speed of the test rig depends on the tested bearing size. Table 2 shows the calculated speed for several bearing sizes at 600,000 NDm and 800,000 NDm.

**Table 2. Bearing speeds**

| Bearing Number | Inner Diameter [mm] | Outer Diameter [mm] | Pitch Diameter [mm] | Speed at 600000 NDm [rpm] | Speed at 800000 NDm [rpm] |
|---|---|---|---|---|---|
| 6204 | 20 | 47 | 33,5 | 17910 | 23880 |
| 6205 | 25 | 52 | 38,5 | 15584 | 20779 |
| 6206 | 30 | 62 | 46 | 13043 | 17391 |
| 6207 | 41 | 66 | 53.5 | 11214 | 14953 |
| 6208 | 40 | 80 | 60 | 10000 | 13333 |

As observed in the table above, the value of speed needed in the test rig are really high which represents a challenge in the selection of components and measurement systems that are able to work at that number of speeds.

Friction Torque

The friction torque generated by a bearing is really small, so selecting a sensor or creating a mechanism that allow measuring the torque in that range will be challenging and represents one of the main risks of the project. Theoretical estimation of the friction torque depends on the bearing type. Different coefficients of friction for different types of bearings are shown in the table below.

**Table 3. Coefficient of Friction for Bearings (American Roller Bearing Company, 2017)**

| **Bearing Type** | **Coefficient of friction - μ** |
|---|---|
| Deep Groove Ball Bearing | .0015 |
| Angular Contact Bearing | .0020 |
| Cylindrical Roller Bearing, Cage | .0010 |
| Cylindrical Roller Bearing, Full Comp. | .0020 |
| Tapered Roller Bearing | .0020 |
| Spherical Roller Bearing | .0020 |
| Ball Thrust Bearing | .0015 |
| Cylindrical Roller Thrust Bearing | .0050 |
| Tapered Roller Thrust Bearing Cage | .0020 |
| Tapered Roller Thrust Bearing Full Comp | .0050 |

As it is shown in the table, these theoretical calculations of friction are very small, and can give a rough idea of the amount of torque that will be measure. However, these values do not consider high values of speeds (as the ones existent in this project), so an estimation of friction torque in needed and it will be developed in Chapter 2 of this document.

Electric Potential

Another main challenge of this project is to generate an electric potential in the shaft and in the bearing. In principle this is not complex, but this complexity increases when the test rig has other functionalities such as loading and measurement torque system. The

challenge in this field will be to apply the potential without affecting other components and measurement system. Another aspect to consider is closing the circuit without introducing additional friction to the system.

## 1.4 Report Outline

This document has been divided in 7 parts which explain the methodology followed in the development of the project until arrive to the concept idea. The first chapter contains the introduction to the problem, the objectives, requirements, and scope of this project. The literature background and research summary are explained in chapter 2. After the deep research of possible solutions for the test rig, chapter 3 shows the explanation of the generation idea phase based on the research, the evolution of the different solutions, and finally the selection of the best concept. Chapter 4 focuses on calculations of the selected design, while chapter 5, 6, and 7 show the summary of the work developed, future activities and recommendations for the following steps in the project.

# 2 BACKGROUND

## 2.1 Existing Test Rigs

To develop a mechanism to test ball bearings with the provided requirements, first research on existing test rigs is conducted. While there are many reports summarizing the mechanism's layout, there are few with details applicable to this project. Sections 2.1.1 to 2.1.4 discuss aspects from test rigs that are presented in the future designs.

### 2.1.1 Start-Stop Journal Bearing Test Rig

A test rig for studying friction and wear in journal bearings was developed as a part of Master's Thesis project at KTH Royal Institute of Technology by Marcus Gralde and Tomas Runar Solvason in 2014. The test rig had mechanisms to apply radial load to the bearings and measure friction torque using housing rotation principle. The torque measurement methodology is based on the Eindhoven test rig developed by Peels and Meesters, 1996. The figure below illustrates the principle of torque measurement in the test rig.

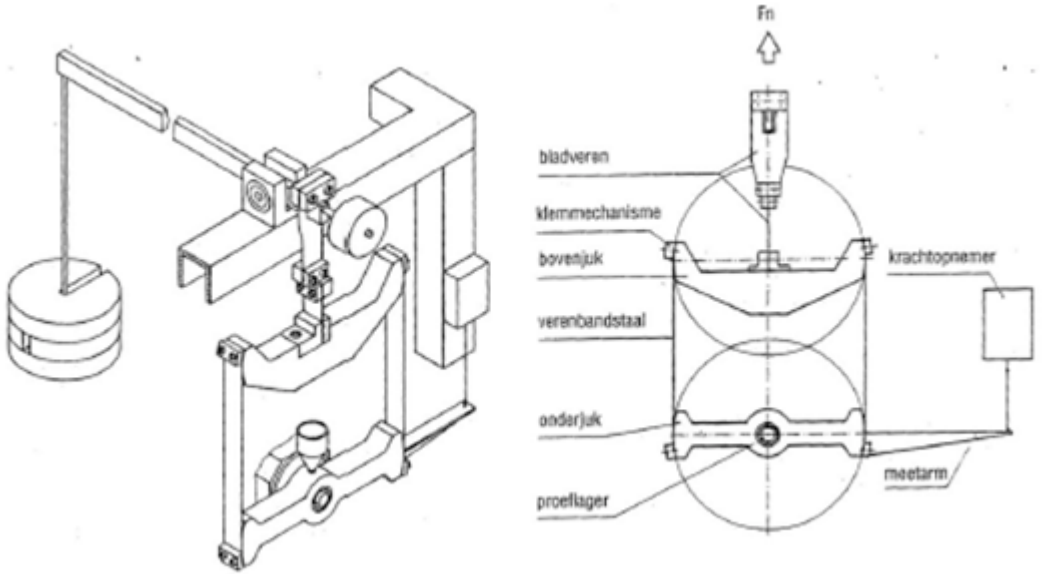


**Figure 3. Principle of Torque Measurement (Gralde, 2014)**

The system employs two yokes that are connected by two thin sheet metal pieces. The two yokes both have radiuses that allow for them to turn, winding up or down the sheet metal around its radius. This allows the yokes to shear when a torque is applied at the bearing, which is measurable with an arm coupled to a force sensor as seen on the right of Figure 3. The test rig employs dead weights to load the bearings.

### 2.1.2 Skf Rof+ Test Rig

Bearing manufacturer SKF developed a test rig for determining the service life of grease lubricated rolling bearings. The rig has flexibility in varying the load, speed, temperature and the bearing type. Pictured below, the ROF+ Test rig has five units, where each unit contains two test bearings.

**Figure 4. ROF + Setup**
(Source: http://www.skf.com/binary/81-65473/The-R0F_plus-methodology-for-grease-life-testing.pdf)

A frequency controlled electrical motor rotates the shaft with test bearings. Pneumatic actuators apply both radial and axial load to the test bearings. The temperature of the grease is monitored until the point where the defined “critical temperature” is reached. The friction torque of the bearings is measured indirectly based on the power consumed by the motor. This testing methodology is used to measure grease performance and to measure the domains in which the grease can successfully function.

### 2.1.3 Bearing Electro Corrosion Tester

The test rig was developed at State Key Laboratory of Tribology at Tsinghua University, China. The rig was constructed to investigate the damage behavior on the lubricated surfaces in bearings with the passage of weak electrical currents as low as 1 mA.

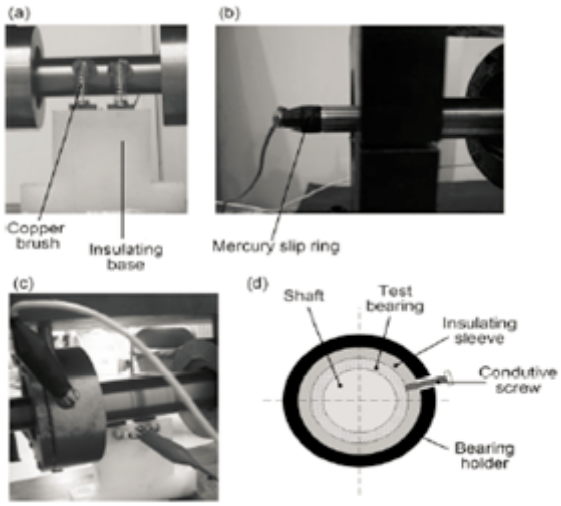


**Figure 5. Applying Electrical Field**
(Source:https://www.researchgate.net/profile/Guoxin_Xie/publication/265088337_Damages_on_the_lubricated_surfaces_in_bearings_under_the_influence_of_weak_electrical_currents/links/53fe74b80cf283c3583bd7d6/Damages-on-the-lubricated-surfaces-in-bearings-under-the-influence-of-weak-electrical-currents.pdf?origin=publication_list)

The above image displays the scheme of applying an electrical field onto the lubricant film in a test bearing. The first two images are the photographs of connecting one pole of a dc power onto the shaft; the lower pair of images is a live photo and the schematic diagram for connecting the other pole of the power onto the outer ring of the bearing, respectively. The rig also had the possibility to apply radial load to the test bearings using a screw-nut principle.

### 2.1.4 Deep Groove Ball Bearing Test Rig

This test rig was developed at School of Mechanical, Electronic and Information Engineering at University of Ming and Technology at China. This rig was developed to test the influence of radial load and rotational speed on friction torque in deep groove ball bearings. Measured friction torque values were correlated with the theoretical SKF torque

model. The key part of the test rig is the integrated loading and torque measurement apparatus.

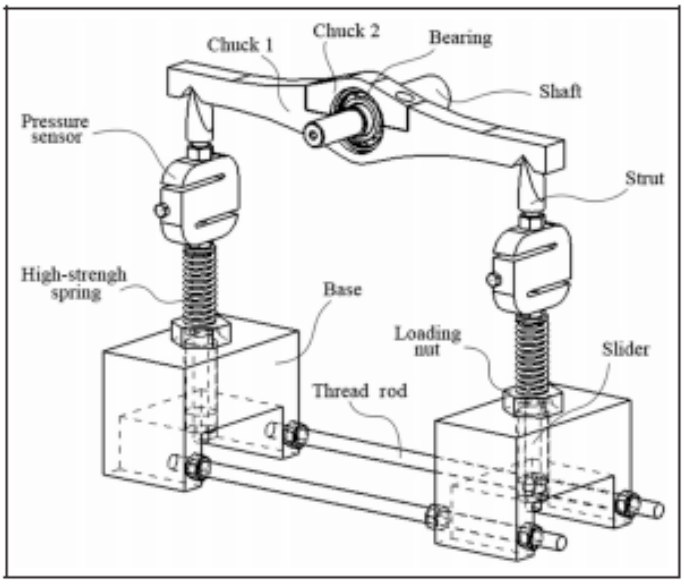


**Figure 6. Loading and Torque Measurement System**
(Source: http://journals.sagepub.com/doi/pdf/10.1177/1687814015586111)

Nut with threaded rod is used to load the bearing. Before measurement, the left and the right loading nuts are tightened to make the load values of the two pressure sensors equal. When the bearing inner ring rotates, there will be a difference in the load values of the two pressure sensors. This difference corresponds to the bearing friction torque.

## 2.2 Friction Torque

One key aspect that differs in test rig concepts is the method to measure the friction in the system. Since there is no completely direct method to measure the total friction in the grease of the test bearing, torque is often utilized as a method to estimate the friction. In this section, the range of friction torque is determined, and then methods to measure torque are described.

### 2.2.1 Torque Estimation

In order to select a torque sensor or design a torque measurement methodology, it is important to estimate the values of friction torques generated in deep groove ball bearings under given conditions of radial load and rotation speed. Bearing manufacturers like SKF

and Schaeffler have created their own theoretical models for estimation based on extensive experimental results. In this work, Schaeffler's calculator is used to estimate the friction torque.

Equation 2: $M_R = M_0 + M_1$

Friction torque as function of speed for $\nu . n$ ≥2000:

*Equation 3:* $M_0 = f_0 \times (\nu . n)^{\frac{2}{3}} * (d_m)^3 * 10^{-7}$

Friction torque as function of speed for $\nu . n$ ≥2000:

*Equation 4:* $M_0 = f_0 \times 160 \times (d_m)^3 \times 10^{-7}$

Friction torque as function of load for ball bearings:

*Equation 5:* $M_1 = f_1 * P_1 \times d_m$

Where

$M_R$ is the total friction torque in Nmm

$M_0$ is the friction torque as function of speed in Nmm

$M_1$ is the friction torque as function of load in Nmm

$n$ is the operational speed of the bearing in rpm

$d_m$ *is the mean bearing diameter in mm*

$f_0$ is the bearing factor for friction torque as function of speed.

$f_1$ is the bearing factor for friction torque as function of load.

$\nu$ is the kinematic viscosity of the lubricant at operating temperature. In the case of grease, the decisive factor is the viscosity of the base oil at operating temperature

$P_1$ is the decisive load for friction torque. $P_1$ is same as the radial load for the case considered.

Bearing factor $f_1$ for deep groove ball bearing is $0.0009 \times (\frac{F_a}{C_0})^{0.5}$

Based on this model, a MATLAB program was developed to estimate torque for all sizes of bearings and under all operating conditions. The following figure displays the calculated friction torque as a function of speed for each bearing size.

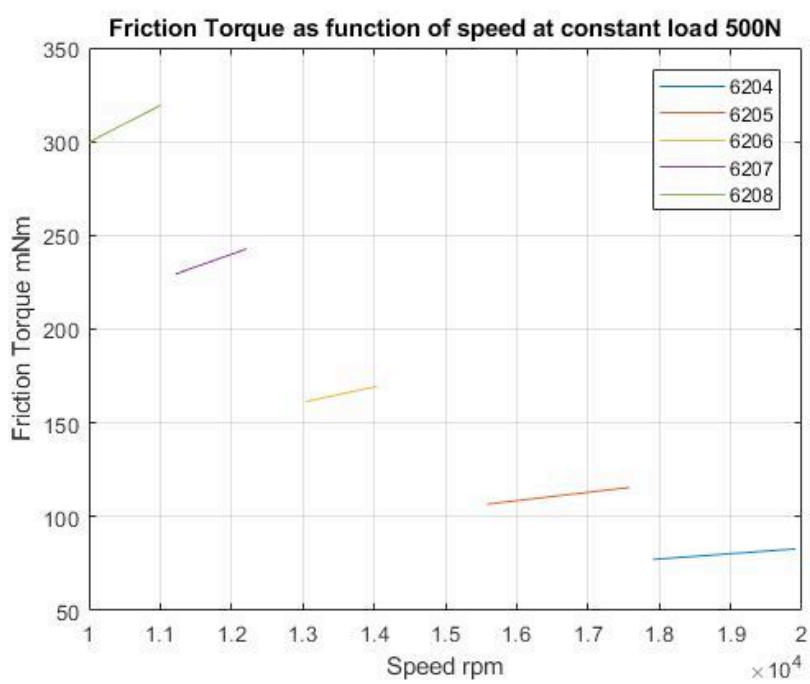


**Figure 7. Friction Torque Range for Each bearing**

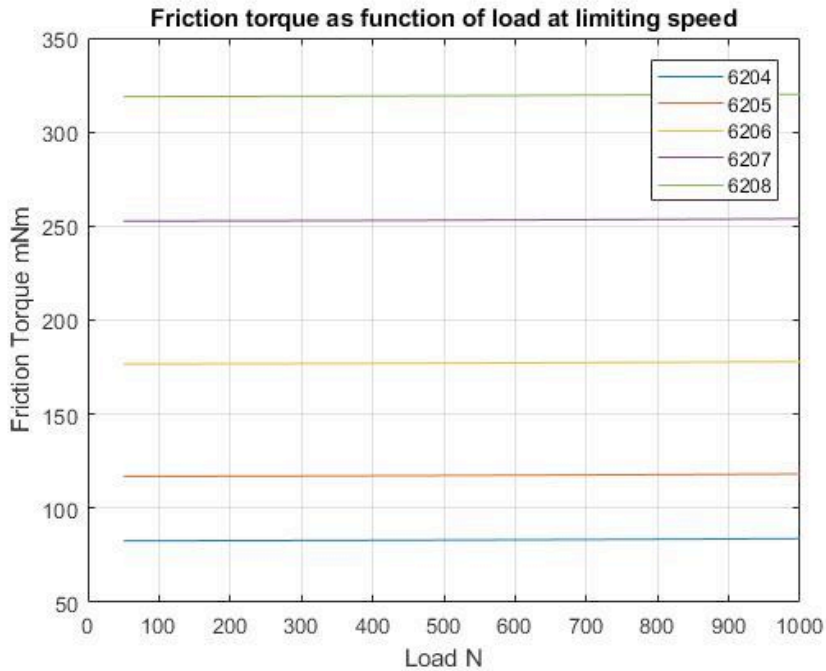


**Figure 8. Friction Torque vs. Applied Load**

The graphs indicate a high dependency of friction torque on speed of rotation. Load seems to play a less significant role in generation of friction torque. Bearing with the biggest size had the highest friction torque.

**Table 4. Friction Torque Range**

| Bearing Number | Lowest Force (N) | Lowest Speed (rpm) | Lowest Torque (mNm) | Highest Force (N) | Highest Speed (rpm) | Highest Torque (mNm) |
|---|---|---|---|---|---|---|
| 6204 | 50 | 17,910 | 76.8 | 200 | 23,880 | 93.1 |
| 6205 | 100 | 15,584 | 106.3 | 400 | 20,779 | 129 |
| 6206 | 150 | 13,043 | 161 | 600 | 17,391 | 195.6 |
| 6207 | 200 | 11,214 | 229 | 800 | 14,953 | 278.3 |
| 6208 | 250 | 10,000 | 299.4 | 1000 | 13,333 | 363.7 |

From the table, the range of torque is about 70 mNm – 400 mNm, depending on the bearing size selected for testing. Due to the complex nature of friction torque, the exact range will be determined through testing in the physical mechanism. The torque estimation assists in determining an appropriate the torque measurement methodology, which will be discussed in upcoming sections.

### 2.2.2 Direct Torque Measurement

There are many types of mechanisms, which can directly measure torque. For the purposes of this project, the research focused on discovering an existing sensor, since creating a torque sensor is not within the scope of the project. The main types of torque sensors that can withstand fairly high speeds and low torque values are described below.

Inline Torque Sensors

Inline torque sensors have two shafts on either side in order to measure the difference between the two ends. The torsion between the two shafts is measured through an internal strain gage. The value of the torque is either displayed on the device or sent wirelessly to a computer. This is a fairly common method for measuring the torque on the shaft and must be directly attached in the shaft.

**Figure 9. Inline Torque Sensor**
(Source: datum.electronics.co.uk)

From the products currently available, some inline torque sensors are able to measure the micro torques with enough sensitivity but are unable to do so at high speeds. This torque sensor is also vulnerable to loading and misalignments in the shaft, which would cause it to malfunction or completely break at the necessary high speeds. In order to determine a more applicable sensor, the focus turned to non-contact sensors.

Magneto-Elastic Torque Sensors

Magneto-elastic sensors utilize non-contact technology to measure parameters like rotational speed or torque with mechanical and magnetic properties. The method involves measuring changes in the properties of the magnetic field by measuring changing mechanical properties like shear stress as external forces are applied to the sensor host. The method directly magnetizes the mechanical member, instead of attaching a ring and a highly sensitive fluxgate sensor is set in close proximity to sense the change in magnetic field characteristics.

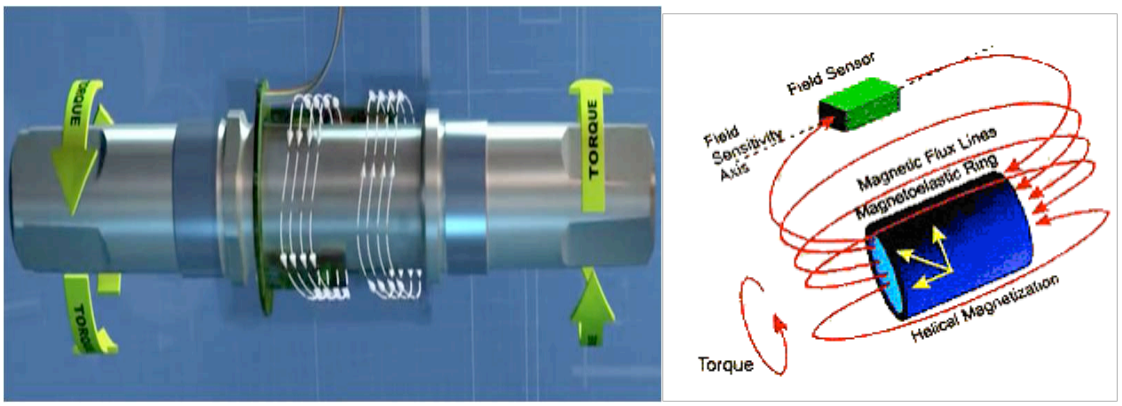


**Figure 10. Magneto-elastic sensor**
(Source: http://www.methode.com/sensors-and-switches/magneto-elastic.html#.WvyT1S-B2Rs)

These sensors can have a range of 0 to +/- 1Nm, resolution of 0.1 Nm to 0.5 Nm, and accuracy of 0.5% to 1.0%. This option may be ideal, except for the rarity of the product and the maximum operating speed is 10,000 rpm. The sensing element is mainly made from martensitic stainless steel, which has great magnetoelastic properties. Several non-contact torque sensors such as eddy current sensors, capacitance, ultrasound, laser, fiber optic sensors were also looked into and were not satisfactory for the micro torques.

OPTICAL ENCODERS

The best option for a non-contact method to measure torque may be through the angle of twist in the shaft between a support bearing and the test bearing. The torque can be estimated with the equation below using the angle of twist, shaft radius, shaft length, and shaft material modulus of rigidity.

*Equation 6:* $$T = \frac{\pi R^4 G}{2L}\Phi$$

Where T is the torsion

R is the shaft radius

L is the shaft length

G is the modulus of rigidity of the shaft

Φ is the angle of twist

To measure the angle of twist of the shaft, two optical sensors are required at either end of the shaft segment. In the image below, the sensors are marked as incoders, which work similarly to transformers.

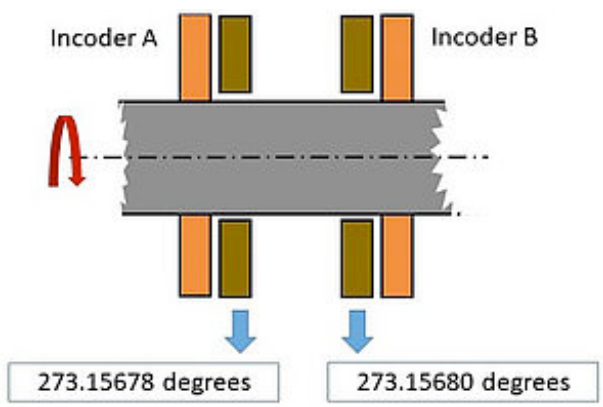


**Figure 11. Optical Sensor Example**
(Source: https://www.zettlex.com/articles/torque-measurement-angle-sensors/)

The best option for measuring angular twist is optical Encoders by Zettlex called IncOders. This utilizes inductive principles to compare the position of the passive Rotor relative to the powered Stator, as pictured below.

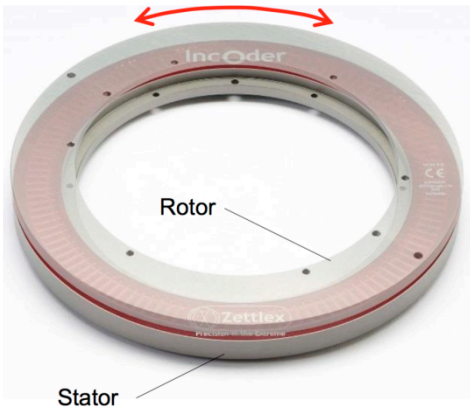


**Figure 12. IncOder**
(Source: https://www.zettlex.com/wp-content/uploads/2014/06/1incoder-product-guide-rev4.09.pdf)

For inner diameter size, the IncOders are available with "mini" from 5.0 to 12.7mm with a resolution of 0.00275mm and with "midi" from 35 to 260mm with a resolution of 0.00017mm. All IncOders have 1% repeatability and 0.27% accuracy, which are ideal for the test rig. In addition, this product is not sensitive to dust/dirt, unlike typical optical sensors.

The key restraint for implementing the IncOder into a design is the limiting speed of 10,000rpm, thus only bearing 6208 at 600,000NDm may be used. Another negative aspect is the maximum allowable misalignment is 0.25mm. In addition, the resolution of the midi-size sensors is 0.00017 degrees. To create a shaft with this angle of twist, a two-material system is necessary. The dimensions of the shaft length and thickness of inner steel shaft and softer outer material must be calculated for designs that implement the IncOders.

### 2.2.3 Indirect Friction Torque Measurement

<u>Load Cells Resisting Rotation</u>

Due to the limiting speeds for direct torque measurement, indirect methods are explored. This concept is relies on load cells to measure the resistive force to keep the bearing from rotating. If placed in a floating housing, the friction in the test bearing would cause a rotation. By measuring the amount of force from the housing to two fixed load cells, the torque may be calculated.

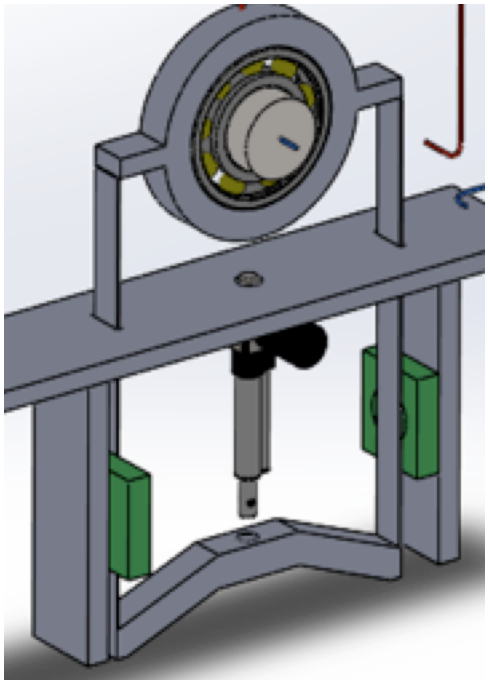

**Figure 13. Loading system structure with load cells**

In the image above, the loading cell system is applied to an actuator loading system component. The green load cells are required to have extremely high sensitivity and accuracy to measure resistance from rotation.

Pressure Sensors For Rotation Force

Measuring the difference in two S-type pressure sensors is another similar method to determine torque. The details of this method are explained earlier in Section 2.1.4.

Beam And Strain Gauge System

Another method to measure torque with a strain gage is through a beam. The layout of this mechanism is pictured below.

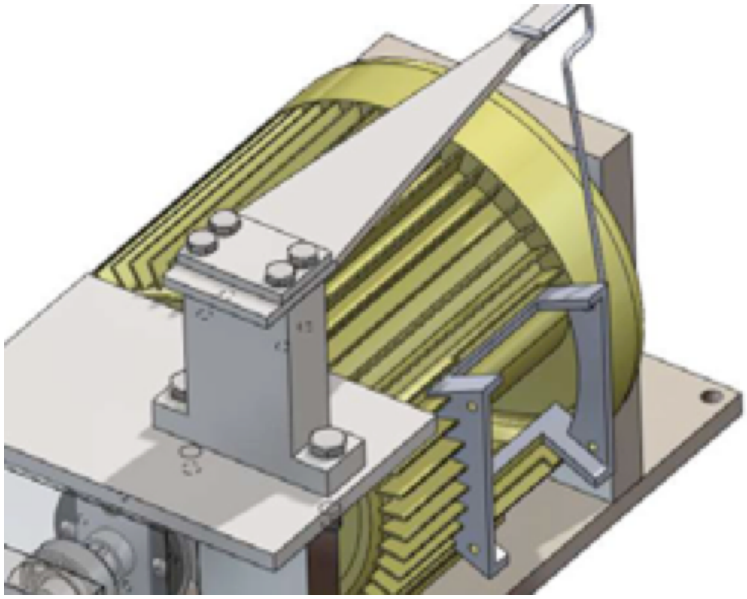

**Figure 14. Arrangement of the beam system**

The beam is located above the electric motor, which is running the shaft; the beam is connected to the motor through a bar that is attached to the motor housing. In this way, the strain gauges located in the beam will measure the displacement in it caused by the rotation force in the electric motor, then the friction torque is calculated from that force.

Motor Current

This concept is based on the brake dynamometer principle where the motor is first run at no-load a calibrated to zero. The shaft rotation is decreased due to the losses experienced. The additional current required to maintain the speed is extrapolated to get the torque value. The value obtained would also have the motor bearing losses and this must be calibrated at the beginning such that the value obtained is only that of the test bearing.

## 2.3 Loading Mechanisms

To simulate the radial loading in an electric motor, the test bearing(s) must be subjected to a range from 50N and 1000N in load. To fulfill this requirement, a device that can apply this range of force, or higher depending on the design layout, is required.

### 2.3.1 Actuators

One of the most common mechanisms to add a force to a system is an actuator. The housing device, pictured below, is based on a test rig described in Section 2.1.1. A model of the unfixed housing is displayed below.

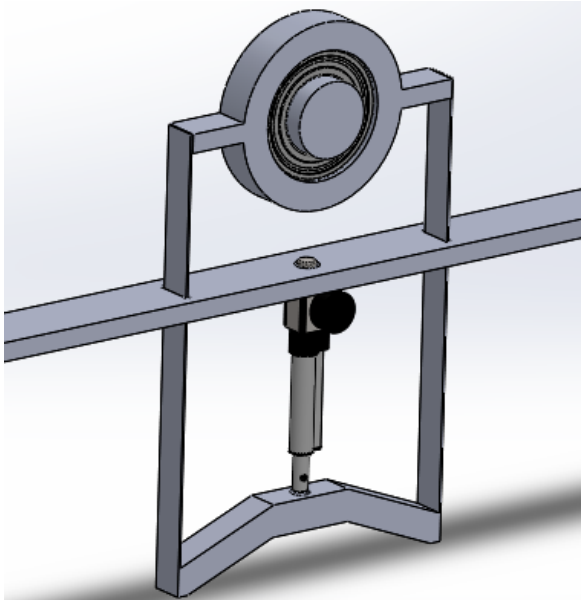

**Figure 15. Loading System Structure**

In this configuration, different types of actuators may be implemented. The two most common actuators are electric and hydraulic. To compare these two options, a chart of advantages and disadvantages was created. The following table displays this comparison to identify the best option for the requirements.

**Table 5. Comparison electric actuators vs hydraulic actuators**

| TYPE | ELECTRIC ACTUATOR | HYDRAULIC ACTUATOR |
|---|---|---|
| PROS | · Flexibility of its motion-control regarding position, velocity, acceleration…<br>· Ease of load variation<br>· Cheaper<br>· Easy to implement | · Great for end-to-end position applications<br>· Good in holding constant load<br>· Able to apply higher loads |
| CONS | · Difficulty in holding a constant load | · Not good at mid-stroke positioning since it requires a control valve system<br>· Problems with leaking, wear<br>· You adjust force by controlling Pressure (more calculations)<br>· Many subsystems & components required for functioning |

The main advantage of a hydraulic actuator is the high loading capacity; however, the complexity of the system and the given range for forces cause hydraulic actuators to not be necessary. Electric actuators are more compact, less expensive, and more appropriate for this project. The main drawback to account for is the difficulty in holding a constant load, as the test rig may run for many consecutive days. To account for this, an electric actuator with a self-locking gear mechanism is selected.

### 2.3.2 Nut and Screw

A popular method to manually apply loading to a system is by a nut and screw. By tightening the nut at the end of a screw, typically attached to a stiff spring then to the desired location, the force on that location is increased. This method involves heavy more calibration than other methods but is ideal if there is electrical current at the loading site.

## 2.4 High Speed Transmission System

A shaft rotating at high speeds (10000-20000 rpm) needs a transmission system a motor that can provide this amount of speed. There are several methods for transmitting the rotational speed from the motor to the driven shaft. Table 6 shows a comparison between

different transmission systems which important design parameters that must be considered during the design process.

**Table 6. Limit parameters of Mechanical Drives (Jelaska, 2012)**

| Drive type | Transmission ratio | Efficiency | Power (MW) | Rotational speed ($min^{-1}$) | Peripheral speed (m/s) | Ratio mass/power (kg/kW) |
|---|---|---|---|---|---|---|
| Cylindrical gears | 45 | 0.99 | 35 | 100 000 | 40 | 0.2 . . . 1.0 |
| Planetary gear trains | 1000 | 0.996 | 65 | 150 000 | 200 | 0.4 . . . 1.8 |
| Bevel gears | 8 | 0.98 | 4 | 50 000 | 130 | 0.6 . . . 2.5 |
| Hypoid gears | 50 | 0.90 | 1 | 20 000 | 50 | 0.7 . . . 3.0 |
| Crossed gears | 100 | 0.95 | 0.08 | 20 000 | 50 | 1.5 . . . 3.0 |
| Flat belt | 20 | 0.98 | 3.6 | 200 000 | 120 | 1.5 . . . 6.0 |
| V-Belt | 15 | 0.94 | 4 | 8000 | 40 | 1.0 . . . 5.0 |
| Worm drives | 100 | 0.98[a] | 1.5 | 50 000 | 70 | 0.2 . . . 4.5 |
| Friction drives | 8 | 0.98[b] | 0.25 | 10 000 | 50 | 8 . . . 30 |
| Chain drives | 15 | 0.99 | 5 | 30 000 | 40 | 6 . . . 10 |

[a] Only for small transmission ratios.

[b] Values are related to planetary friction drives.

### 2.4.1 Belt Transmission System

Belt transmission systems can be classified in timing belts, V-belts and flat belts based on the shape of their section. Each of these options offers different characteristics especially in speed, slipping and stretching. For instance, based on the recommended speeds, flat belt drives are considered a better option than timing or V belts. Table 7 shows the advantages and disadvantages of belt transmission systems in order to show the applicability of them in this project. (Mechanical, 2018)

**Table 7. Flat belts, Advantages and Disadvantages**

| Advantages of flat belts | Disadvantages of flat belts |
|---|---|
| Higher speed limits (flat belts better than timing and V-belts) | Angular velocity ratio is not always constant or equal to the ratio of pulley diameters (except timing belts) |
| Simple installation and economical | Limited power transmission (not important for this project) |
| Protect the shaft or the motor from overload | Low operating temperatures (up to 80 degrees) |
| Misalignments in the shafts can be compensated | Maintenance and adjustment are needed because of wear |
| They act as damping mechanisms | Pretension mechanisms are needed |
| Allows shaft far apart | |

### 2.4.2 High Speed Motors-Shaft Coupling

In addition to some transmission methods used in high-speed applications, the shaft can be connected directly with the motor shaft by an elastic coupling. Figure 17 shows a typical motor-shaft the motor directly applies connection where the velocity needed in the shaft.

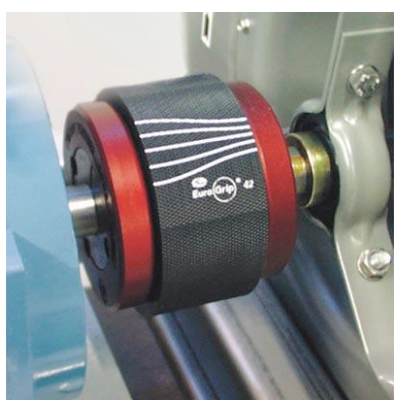

**Figure 16. Elastic Coupling (Beeline Engineering Group, 2018)**

Elastic couplings have the advantage of compensating for misalignments and axial motion in the transmission mechanisms. This characteristic is extremely important at the moment of having high speeds because an extra inertia force could lead to resonances in the

system. Elastic couplings and their damping characteristics allow having higher tolerances, resulting in lower manufacturing. However, this type of connection will imply to select a higher speed motor because the transmission ratio between the driven shaft and the driving motor is one.

High-speed motors with large shaft diameter can be obtained by a high-speed synchronous motor. They are able to provide wide range of constant power, cooling system, and a simplified integration into the machine. This kind of motors, allow having a controlled system (rpm) based on the feedback that the proper motor gives to the drive controller. The following figure shows the parts of the motor and the inter relations between the motor components.

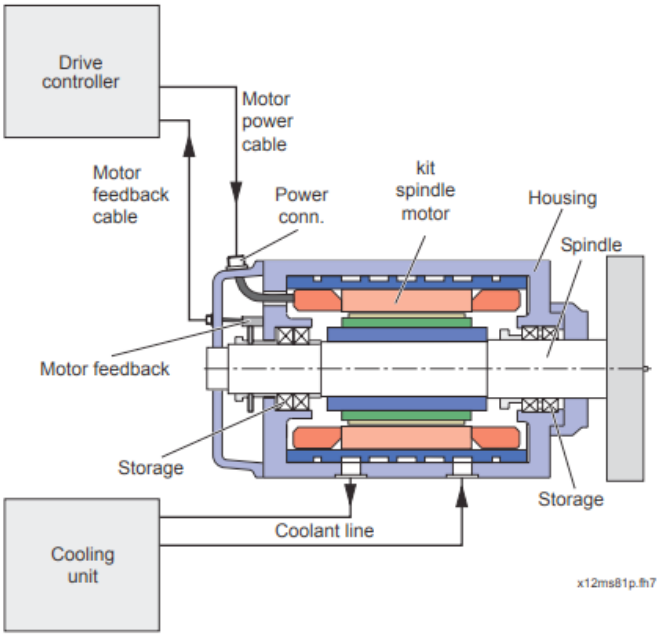


**Figure 18. Motor Components**
(Source: https://www.boschrexroth.com/ics/cat/?cat=Electric-Drives-and-Controls-Catalog&m=XC&u=si&o=Desktop&p=p783135&pi=1B45AD3B-D64F-EE93-55C4469D31324E26_ICS_82)

The following shows several models of Rexroth motors that satisfy the speeds needed in this project. However, its selection will depend on the transmission system and the configuration designed.

**Table 8. Rexroth Motor Specifications**

| **Type** | | **MSS102B-0800** | **MSS102D-0800** | **MSS102F-0300** | **MSS102F-0800** |
|---|---|---|---|---|---|
| **Maximum speed $n_{Max}$** | rpm | 22500 | 22500 | 18000 | 22500 |
| **Standstill torque $M_0$** | Nm | 10.7 | 20 | 32 | 26 |
| **Maximum torque $M_{Max}$** | Nm | 36.7 | 45 | 75 | 68 |
| **Standstill continuous current $I_0$** | A | 16.9 | 24 | 15.3 | 43 |
| **Maximum current $I_{Max}$** | A | 52 | 69 | 35 | 100 |
| **Moment of inertia J [1)]** | kg·m² | 0.003 | 0.004 | 0.006 | 0.006 |

## 2.5 Temperature Measurement

Platinum resistance thermometers (PRTs) offer excellent accuracy over a wide temperature range (from –200 to +850 °C). The principle of operation is to measure the resistance of a platinum element. The most common type (PT100) has a resistance of 100 ohms at 0 °C and 138.4 ohms at 100 °C. There are also PT1000 sensors that have a resistance of 1000 ohms at 0 °C. The relationship between temperature and resistance is approximately linear over a small temperature range.

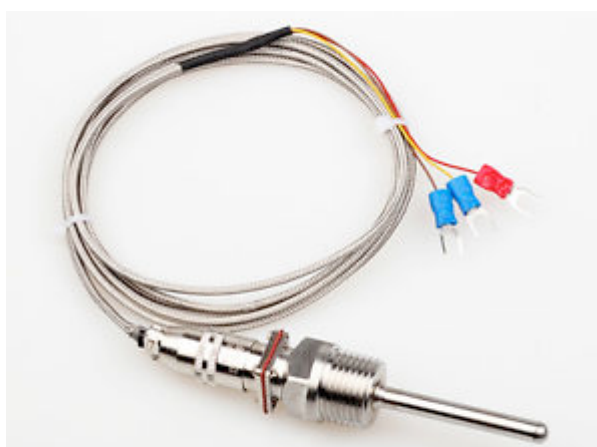

**Figure 19. PT100**
(Source: https://www.ebay.com/itm/RTD-Pt100-Temperature-Sensor-Probe-L-5cm-1-2-NPT-Thread-w-Detachable-Connector-/152834067243)

For a PT100 sensor, a 1 °C temperature change will cause a 0.384 ohm change in resistance, so even a small error in measurement of the resistance, such as the resistance of

the wires leading to the sensor, can cause a large error in the measurement of the temperature.

## 2.6 Electric Potential

This section briefly describes the necessary components and methods to apply an electric potential across the test bearing. This system should realize two main requirements: to apply an electric potential of 1- 2 Volts both AC and DC signal across the test bearing and to isolate the current signal from other components in the test rig.

### 2.6.1 Power Supply

A power supply is an electrical device that supplies electric power to an electrical load. The primary function of a power supply is to convert electric current from a source to the correct voltage, current, and frequency to power the load. A DC power supply applies a constant DC-type voltage to its load. An AC power supply takes the voltage from a wall outlet and uses a transformer to step up or step down the voltage to the desired voltage.

In addition to the voltage type, there is variation in functions of a power supply. An adjustable regulated power supply is both adjustable and regulated. It maintains constant output voltage or current despite variations in load current or input voltage. The output voltage or current can be programmed by mechanical controls (e.g., knobs on the power supply front panel), or by means of a control input, or both.

A programmable power supply is allows remote control of its operation through an analog input or digital interface such as RS232 or GPIB. Controlled properties may include voltage, current, and in the case of AC output power supplies, frequency. They are used in a wide variety of applications, including automated equipment testing. Programmable power supplies typically employ an integral microcomputer to control and monitor power supply operation.

An uninterruptible power supply (UPS) takes its power from two or more sources simultaneously. It is usually powered directly from the AC mains, while simultaneously charging a storage battery. Should there be a dropout or failure of the mains, the battery instantly takes over so that the load never experiences an interruption.

### 2.6.2 Signal Generator

A signal generator is piece of test equipment that produces an electrical signal in the form of a wave. There are several types available to generate a variety of output signals and waveforms.

**Table 9. Signal Generation**

| Types | Function |
|---|---|
| Arbitrary waveform generator (AWG) | Creates very sophisticated waveforms that can be specified by the user. |
| Function generator | Used to generate simple repetitive waveforms |
| Pulse generator | Can produce pulses with variable delays and some even offer variable rise and fall times |
| RF signal generator | Used to generate radio frequency signals. |

(Source: http://www.radio-electronics.com/info/t_and_m/generators/signal-generator-types.php)

The most relevant for our purpose is the function generator. AWG could work as well but it is more complex and expensive relatively. A Function Generator can produce waveforms or functions such as sine waves, saw tooth waveforms, square and triangular waveforms. Typically, it may be able to vary the characteristics of the waveforms, changing the length of the pulse, i.e. the mark space ratio, or the ramps of the different edges of a saw tooth waveform.

### 2.6.3 Isolation Of Current

The applied electric signal has to be kept only across the test bearing so that it does not affect other components and sensors. A simple mechanism to avoid stray current from and to the motor is a coupling device. In order to insulate the current to only the test bearing on the shaft, an isolative sleeve system may be necessary. The approach is to mount a non-conductive sleeve (blue sleeve in figure) onto the shaft and then mount another conductive sleeve on it.

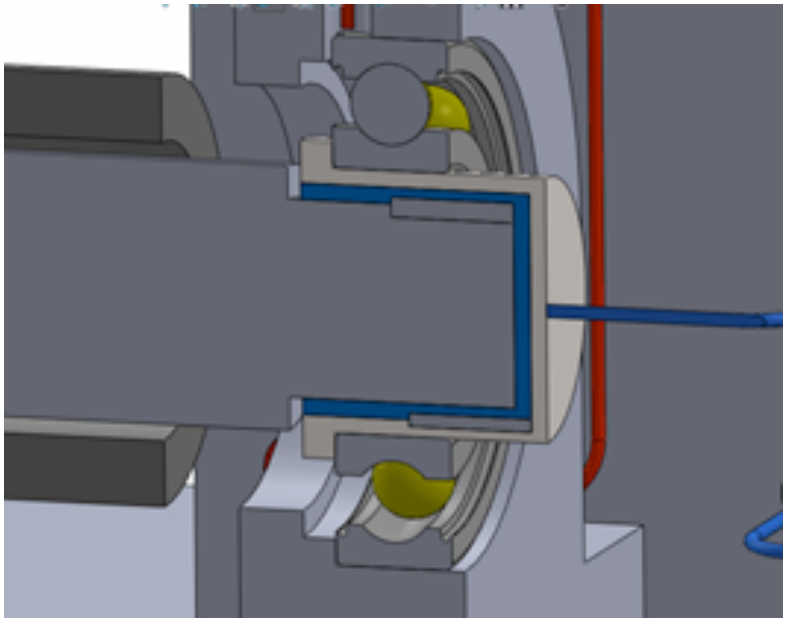

**Figure 20. Non-Conductive Sleeve System**

It can be seen from the figure that electric signal can flow only across the top conductive sleeve. The sleeves are either attached by two keyways or splines, depending on the requirement for the press fit based on the design.

### 2.6.4 Voltage Controlled Resistor (Vcr)

The main purpose of this device is to vary the resistance across a component based on voltage across a section. By controlling the resistance across each test bearing it can be ensured that, an equal electric potential is applied across all sections needed. It is a three-terminal active device with one input port and two output ports.

### 2.6.5 Electric Circuit

The first point of contact for the electric circuit is at the bearing outer ring, which is a stationary contact. The circuit is closed as a point contact at the end of the shaft by means of a brush.

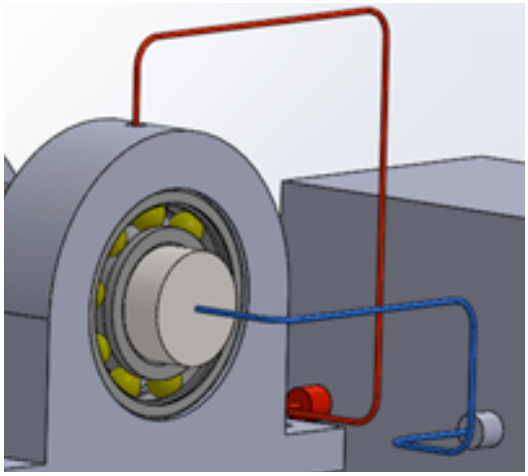

**Figure 21. Electric Circuit with Point Contact**

Closing the circuit as mentioned was the most feasible way, as it would not generate any additional friction torque in the shaft. And compared to brushes across the shaft, it is efficient is terms of stability and wear.

## 2.7 Bearing Seals

### 2.7.1 Antifriction Contact Seals

The Nilos Ring is an anti-friction seal type by SKF bearings and provides practical protection for ball and roller bearings against contamination by dirt and debris, including tough abrasive particles that can cause equipment to malfunction and productivity to be lost. These all-metal seals are ideal for grease-lubricated anti-friction bearings in industrial environments that routinely generate excessive contaminants. The two standard styles of NILOS-Rings for ball bearings and straight (non-tapered) roller bearings are type AV for sealing a bearings outer ring and type JV for sealing a bearings inner ring.

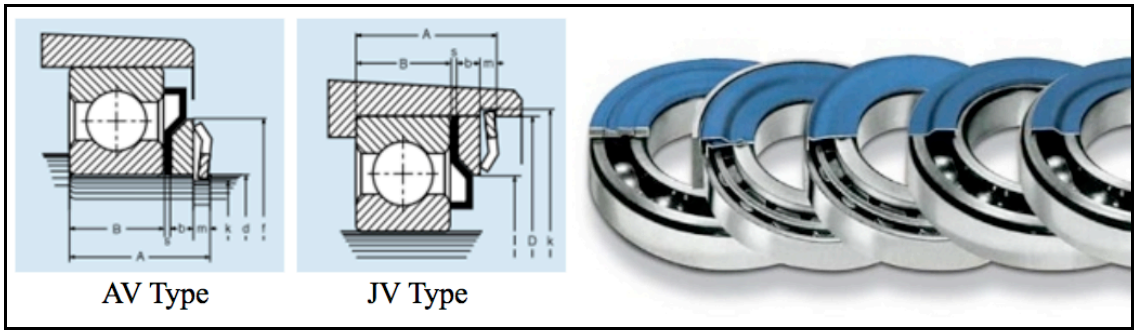


**Figure 22. NILOS-Rings**
(Source: http://www.skf.com/binary/30-228382/950-710-Nilos_08.pdf)

The sealing listed above is an anti-friction sealing, which is mainly taken for single row deep-groove ball bearing. These seals can be used for speeds only up to 6 m/s, thus this type of seal is not permissible for the high speeds of the test rig shaft.

### 2.7.2 Centritec Non-Contact Seals

The Centritec seal utilizes centrifugal method where the bearing rotation causes pressure to pump the lubricant into the bearing and back into the fluid reservoir. The design utilizes a rotating chamber within the seal to create a pressurized barrier as the lubricating fluid exits the chamber.

Since there is no contact between the rotating inner and outer and stationary outer elements, there is high tolerance to vibrations. These seals are designed for custom applications and are applicable at the required speeds. The only concern of these non-contact seals is the price; however, cost is not considered in the design stages.

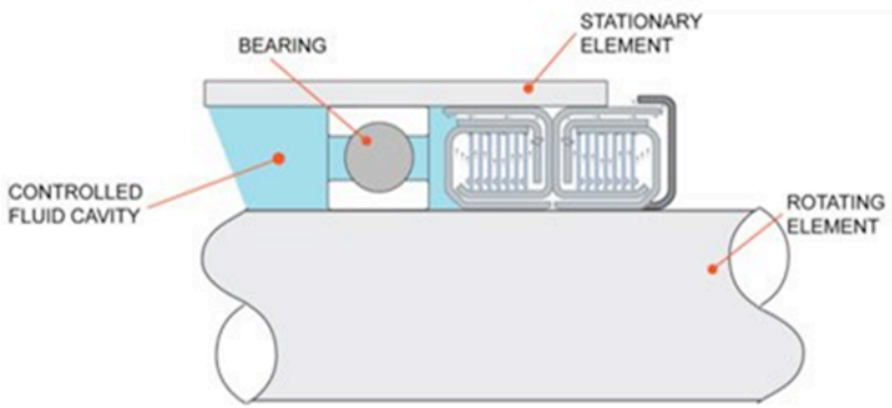


**Figure 23. Centritec Sealing Mechanism**
(Source: https://www.centritecseals.com/non-contact-seals.php)

There are several types of non-contact seals like press mount, slip mount, flange mount ring & slip mount shaft, split seal, closed at rest seal, vertical mount seal and custom seals. The most recommended seal is the flange mount ring and slip mount shaft.

# 3 DESIGNS

## 3.1 Initial Concepts

During the process of conducting the technical background research, the first design concepts were created. Team members individually developed preliminary test rig sketches for layouts with possible combinations of various transmission systems, electric current methods, loading mechanisms, torque measurement techniques, etc. Components from this initial brainstorming process are utilized in many of the refined concepts.

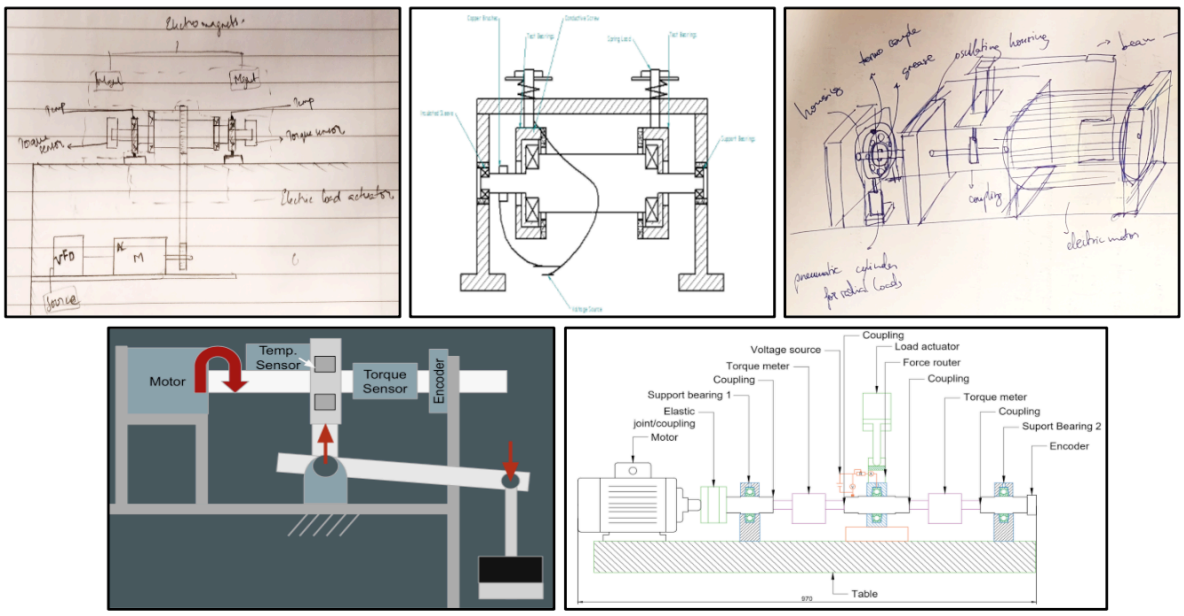


**Figure 24. Initial Concept Sketches**

In the figure above, the first two sketches involve a symmetrical approach with two test bearings and a central pulley transmission system. This concept is explored further in Design C (Section 3.2.3). The other concepts involve one test bearing and are driven directly from a motor, which is assumed to reach the required speeds up to 24,000rpm. The least developed aspect of these concepts is applying and isolating the electric current to the device. While one concept relies on electromagnets, the majority simply introduces the current through the bearing housing. The circuit is closed through a brush on the outside of the shaft, which is not desired since extra friction is introduced.

For the loading mechanisms, three concepts involve actuator acting on the housing of the test bearing. The other sketches implement mechanical loading by the screw and nut method and deadweight mechanism. Loading the bearing housing through an actuator allows more automatic control when testing the bearings, so the mechanical loading options are not continued in future concepts. The next major component is measuring the friction torque due to the friction in the test bearing. One design involves an indirect torque measurement system through strain gages on a beam. The remaining four concepts rely on in-line torque sensors; however, research led to the conclusion that this type of sensor does not function for the required speed and torque ranges. Alternative friction torque sensors are implemented in the refined concepts.

## 3.2 Refined Concepts

The main focus of this project is identifying the best combination of equipment to complete the project goal with the given requirements. To achieve this, the design process involves an evolutionary nature. This segment of the report contains the layout of components in each of the five refined concepts. Each design includes temperature measurement at the outer raceway of the bearing with a PT100, contactless Centritec bearing seals, and a signal generator to apply voltage.

### 3.2.1 Design A: Cantilever Concept

The first major design involves one test bearing in a floating housing cantilever layout. The 2D model of this concept is pictured below and contains a motor connected to the shaft with a coupling, two support bearings, a non-contact torque sensor, and floating housing. This housing contains the test bearing, electric current system, and loading mechanism. Another component pictured is the electric current system. This design utilizes a non-conductive sleeve system and a point contact to close the circuit.

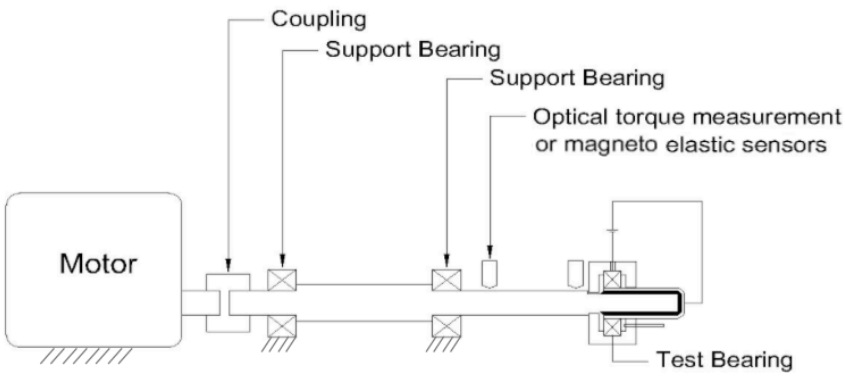


**Figure 25. Design A Layout**

The main issue with this design is the high-speed requirement. As described in section 2.2.2, there are not many direct torque sensors that can apply for the speeds necessary. The best option is torque measurement with IncOders, which require a long, thin shaft to maximize the angle of twist. The following figure displays the static forces on the shaft, as well as the dimensions necessary to implement the optical angular twist sensors.

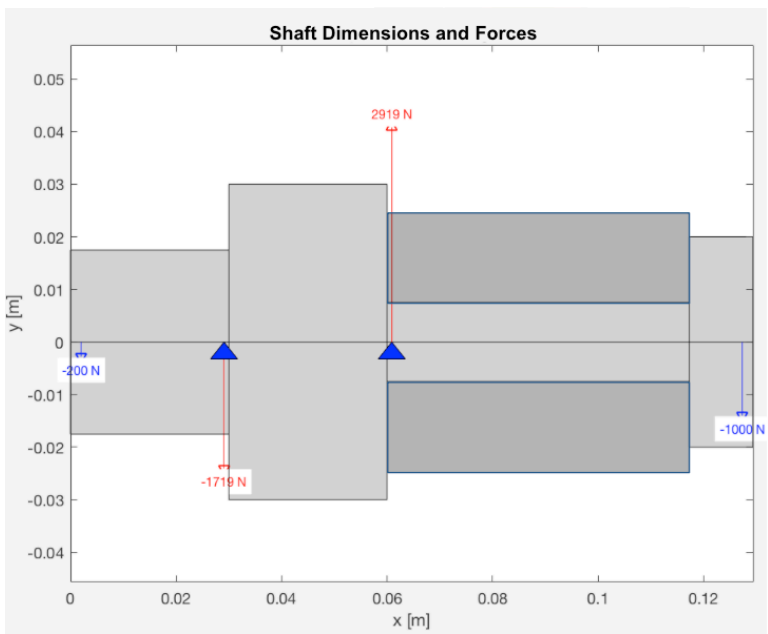


**Figure 26. Design A Dimensions and Forces**

The third step consists of two materials: an inner shaft of steel to decrease deflection and an outer layer, shown in dark grey, of rubber to increase the angle of twist. This 47.3mm long segment has a 15mm inner shaft diameter, 35mm thick rubber layer, and deflection of 0.083mm (Appendix A). Although this setup would allow the use of

IncOders, it is only applicable to bearing 6208 and would only run at 600,000ndm due to the IncOder's limitations. There is also concern of instability in the shaft causing unwanted misalignment and additional fatigue

### 3.2.2 Design B: Central Loading

To reduce the possible misalignment of the shaft, Design B has the test bearing fixed to the table. This design necessitates only one support bearing and the floating loading mechanism is located between the supports. The loading applied by the actuator is now distributed between the two bearings, thus a greater load must be applied. This design also includes the nonconductive sleeve system with a point contact. Unlike Design A, this design is driven by a timing belt system to increase the rotational speed.

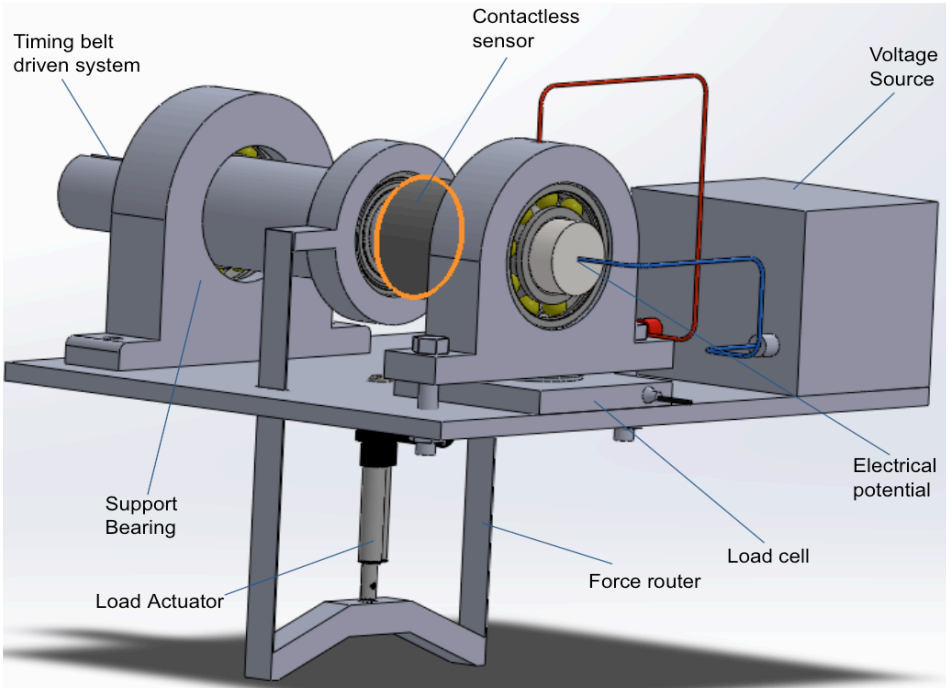


**Figure 27. Design B Layout**

To determine the friction torque, there is a non-contact optical angular twist sensor between the loading and the test bearing on the shaft. The required dimensions for this shaft segment are the same as in Design A.

### 3.2.3 Design C: Two Test Bearings

To ensure a better stability and compact design, a symmetric layout with two test bearings is designed. This design tests two test bearings, which are located in fixed housings on either ends of the shaft. As it can be seen from the figure, the shaft is driven by a belt drive through a pulley located on the center of the shaft. It has a symmetric design and is stable. The dimensions of the shaft are based on bearing selected, so scaling the mechanism can allow for multiple shafts to test multiple bearing sizes.

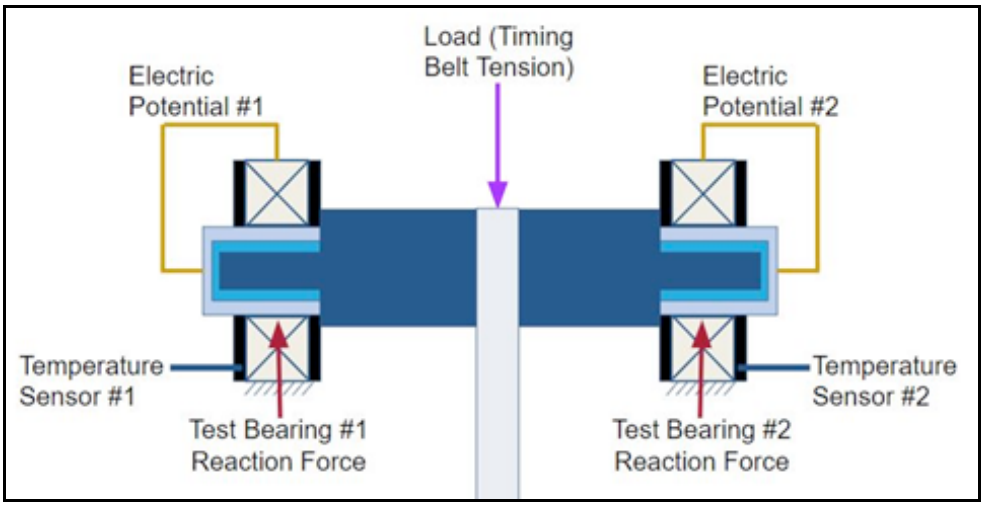


**Figure 28. Design C Layout**

The load onto the test bearings is applied through tension in the drive belt. To change the load, tensioner pulleys control the belt tension. Electric potential application is done using the power supply, function generator and electric circuit described in the above sections. The sleeve arrangement is used to isolate the electric signal to the test bearings.

The friction torque is measured through an indirect method by estimating motor current. The measured value of friction torque is the average of the two test bearings. As the level of friction torque a single bearing generates is very low (milli-Nm), testing two bearings gives a better friction torque estimate. One the main issue in this design is ensuring that no other sources of friction torque except that from test bearings are measured. Another concern is designing a stable loading without affecting friction torque in motor bearing and tensioner pulleys.

### 3.2.4 Design D: Four Test Bearings

Continuing with the multiple test bearing concept, this design tests four bearings of the same size. The two bearings at the ends of the shaft are located in fixed housing acting also as support bearings for the shaft. The two middle bearings are located symmetrically in the middle of the shaft and are located by retaining rings. The test rig shaft is directly coupled to a high-speed motor by means of an elastic coupling.

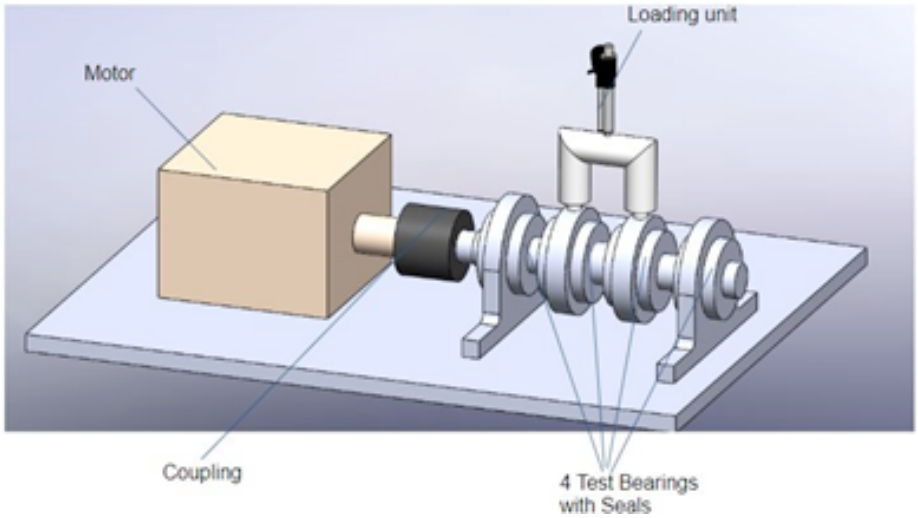


**Figure 29. Design D Layout**

The bearings are loaded through a custom loading structure and a load actuator. The outer rings of bearings in the middle are encased in a circular house. The circular house has slot on top of it to accommodate an inverted U-shaped loading structure. A load actuator is used to apply load on the structure, which loads all the bearings equally due to the symmetric arrangement. Electric potential application and closing of the circuit is done as in previous designs, but the use of four bearings necessitates an additional system. A VCR is used to maintain a constant resistance across the bearings based on the voltage level across a bearing. This is to ensure that all test bearings have equal potential across them. The friction torque is measured through an indirect method by estimating motor current as in the previous case. With direct coupling, the issue of adding friction with a pulley is eliminated, but this also decreases the safety of the device and requires a motor that can reach the top speeds. The measured value of friction torque is the average of the four test bearings.

### 3.2.5 Design E: Advanced Cantilever

The need for a simple yet effective configuration to apply load to the test bearing and measure friction torque was felt despite generating many concepts for the test rig. These requirements are met in this concept named "Advanced Cantilever".

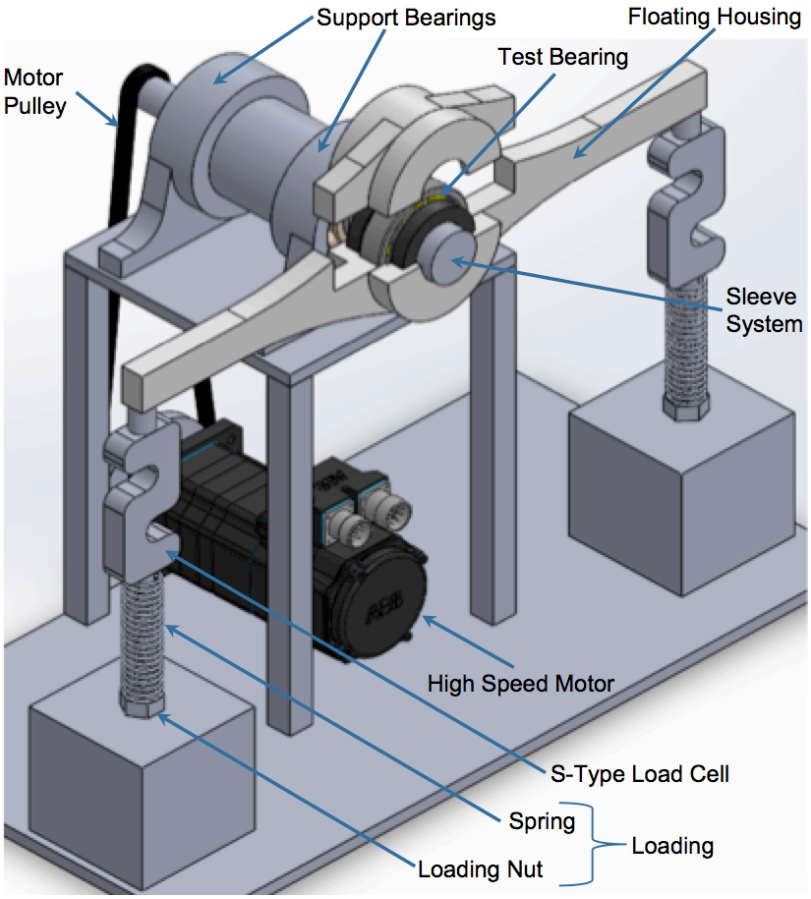


**Figure 30. Design E Layout**

Friction torque is measured through the rotation of housings with S-type load cells. The test bearing is cantilevered in a floating housing with two horizontal arms. The radial load to the bearings is applied through a screw and nut principle that applies load to the bearing through the loading arms. A load cell is kept in between the arm of the housing and source of load. A high strength spring is also used in the loading arrangement in order to take care of impact loads generated at the test bearing from being propagated back to the loading screws.

These measures both the applied load as well as the difference in loads between two arms of the load cell generated because of friction torque in the bearings. As can be seen the design incorporates a cantilever arrangement for loading the test bearing. The drive arrangement for this design is same as many of the previous concepts where a motor with pulley is used to drive the shafts.

## 3.3 Design Evaluation

Due to the evolutionary process of the design, the latest concept, Design E, could be the best solution to achieve the project objectives, but the complex nature of the mechanisms condones a comparison between each of the designs to determine the final design.

### 3.3.1 Morphological Chart

To compare the designs, first the components of each option must be identified. In the Morphological Chart below, each of the initial concepts and refined concepts are represented by arrows to identify which designs involve the possible options.

**Concept Path Key**

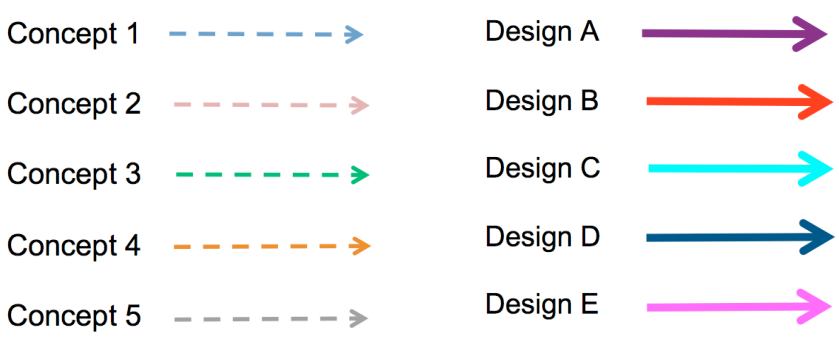


(see following page)

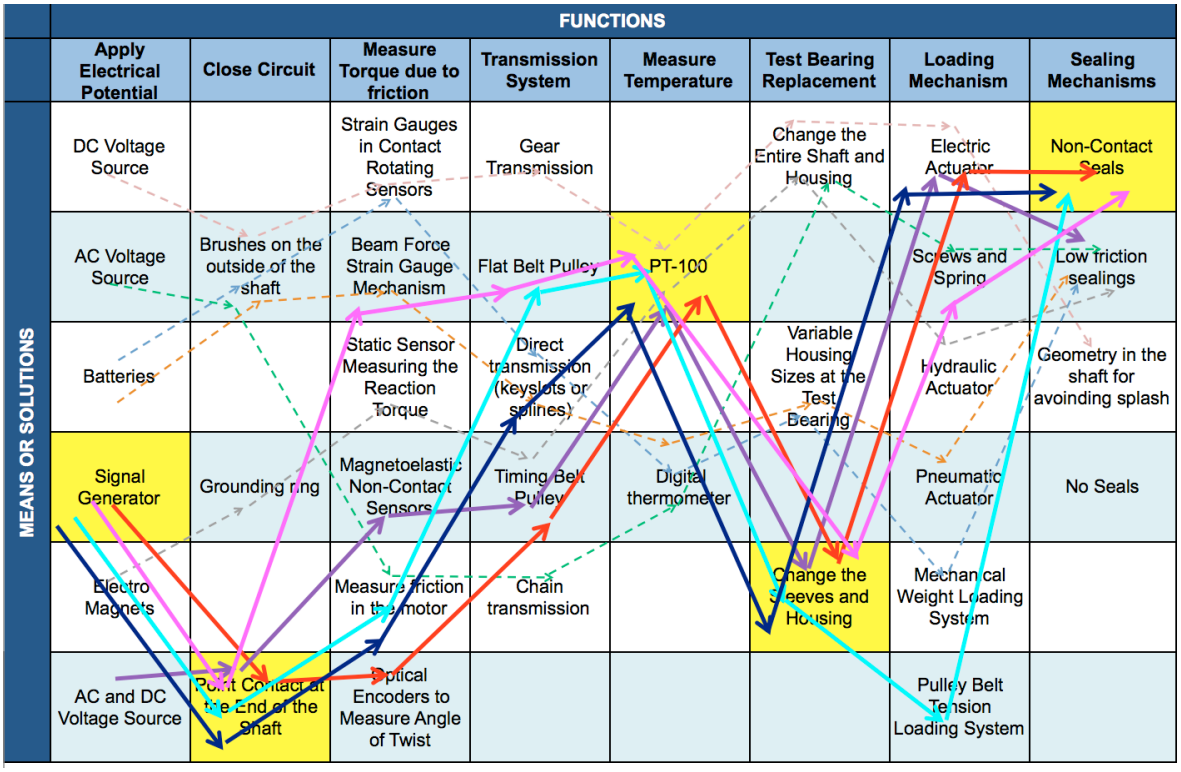


**Figure 31. Morphological Chart**

The thin lines indicate the initial concepts and the bold arrows correlate to the advanced designs. The chart displays the variation in solutions for each aspect of the project; however, there are many options and many designs in this diagram. To solely compare aspects of the refined concepts, Appendix C contains a table containing a summary of the components in Designs A to E.

### 3.3.2 Pugh's Matrix

As previously identified, some designs do not fulfill all of the project requirements, especially the initial concepts. Because of this, only the more developed concepts are compared to identify the optimal layout for the test rig. The following weighted Pugh's Matrix compares the designs to Design E, since this concept is most likely the best solution.

| Criteria | Weight | Design E | Design D 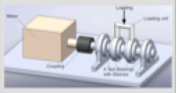 | Design C 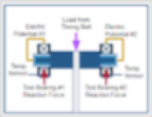 | Design B 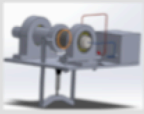 | Design A 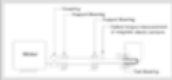 |
|---|---|---|---|---|---|---|
| Electric Potential System | 5 | R | 0 | 0 | 0 | 0 |
| Friction Torque Measurement | 5 | E | 0 | 0 | -1 | -1 |
| Grease Temperature Measurement | 4 | F | 0 | 0 | 0 | 0 |
| Applying Speed of 800.000 nDm | 4 | E | 0 | 0 | -1 | -1 |
| Variation in Shaft Speed | 3 | R | 0 | 0 | 0 | 0 |
| Loading Mechanism | 2 | E | 0 | -1 | 0 | 0 |
| Bearing Size Versitality | 1 | N | 0 | 0 | -1 | -1 |
| Ease of Disassembly | 3 | C | -1 | -1 | 0 | 0 |
| Stability and Safety | 3 | E | 0 | 0 | 0 | -1 |
| **TOTAL** | | **0** | **-3** | **-5** | **-10** | **-13** |

**Figure 32. Weighted Pugh's Matrix**

It is interesting that the designs did progressively improve as the project developed. As each of the designs preceding Design E has a score below zero, the advanced cantilever design was confirmed as the best mechanism configuration.

# 4 ANALYSIS

## 4.1 Static Analysis

For the final design considered, static analysis was carried out using a MATLAB code developed by Stefan Björklund from Machine Design department at KTH Royal Institute of Technology (Appendix B). The code has been applied to the layout of Design E and provides a neat visualization of the reaction forces. The program also calculates the shaft deflections, angular misalignments at supports and the stresses induced in shaft.

### 4.1.1 Forces

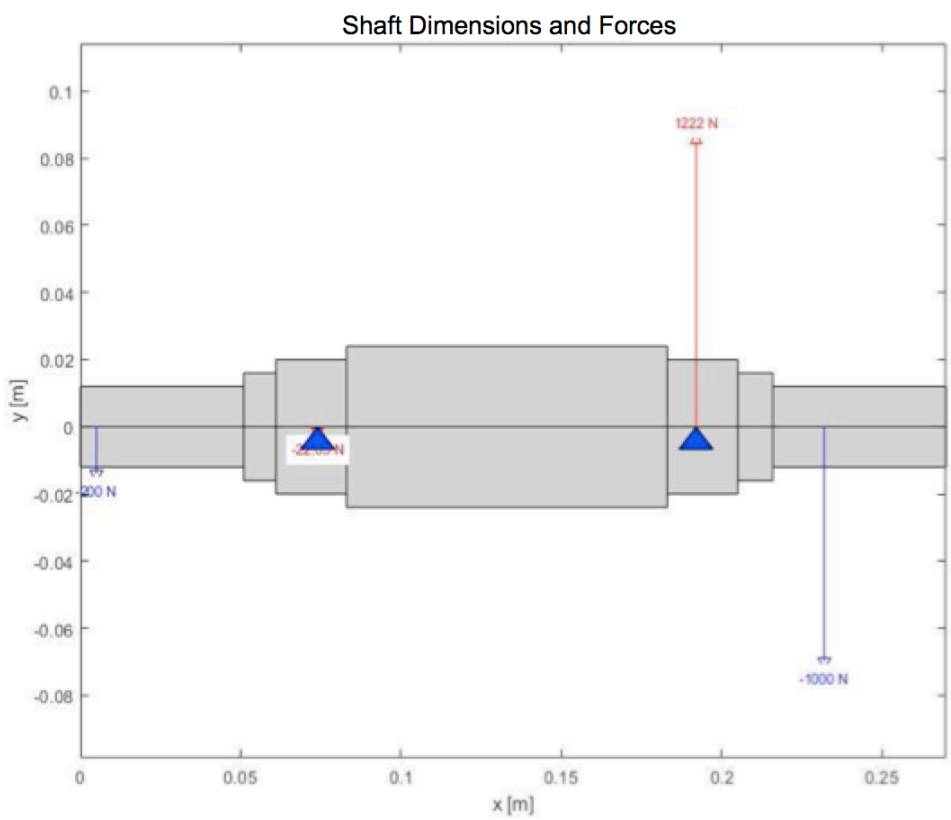


**Figure 33. Shaft Dimensions and Forces for Design E**

One aspect to note is a relatively high force at the second support bearing with the current dimensions. This was identified as not an issue because the load capacity of the chosen support bearing is much greater. An assumption involved in this calculation was that the pulley belt tension is 200 N. This was a rough approximation taken keeping in

mind the reduction ratio of the pulley and the total shaft friction. Further development of the optimal shaft dimensions and updated pulley force will be included in future work.

### *4.1.2* Static Stresses, Slope, And Deflection

The program also calculates the static stresses, slope and deflections, which are displayed in the following image.

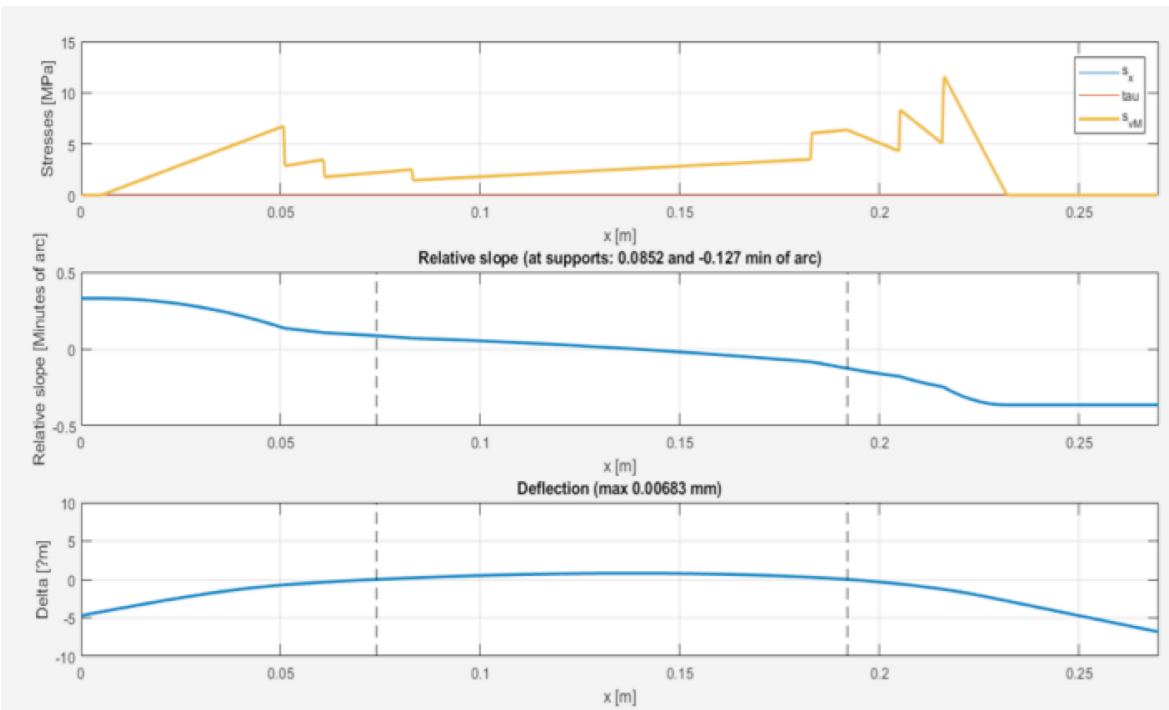


**Figure 34. Stresses, Slope, and Deflection of Design E**

Angular misalignment generated at bearing supports doesn't exceed the critical limit of the bearing. Maximum deflection is generated at the location of the test bearing because of the cantilever arrangement. This deflection is 0.00683mm in a static system and may increase when the high speeds are applied. In the future, the design will be evaluated in detail with a dynamic analysis to consider fatigue life.

## 4.2 Dynamic Analysis

### 4.2.1 Critical Speed

The critical speed is the theoretical angular velocity, which excites the natural frequency of a rotating shaft. It is estimated using the Rayleigh-Ritz method; the calculated value gives an estimate as to in which range the critical speed lies.

*Equation 7:*

$$Nc = \frac{30}{\pi} \times \sqrt{\frac{g}{\delta st}}$$

Where N is the critical speed in rotation per minute

g is the acceleration due to gravity

$\delta$st is the maximum static deflection in meters

The static analysis for Design E calculated a maximum deflection in the shaft as 0. 00683 mm. The calculated critical speed for a shaft dimensioned based on 6208 bearing for Design E is 11,442 rpm. This value is the first approximation of the critical speed, which should be avoided if possible. A more detailed calculation of critical speed will be conducted with the optimized dimensions.

# 5 CONCLUSION

Friction torque in bearings is challenging to measure and most commercially available sensors cannot be used due to the high rotational speed requirements in the test rig. Innovative techniques are required to use the available standard equipment in the market and design an indirect torque measurement methodology.

The project resulted in a solution that satisfies all of the requirements for a test rig. Conductive greases are an innovative solution to avoid bearing failure due to electric discharge in electric machinery. This test rig will be the first of its kind as it provides various functionalities simultaneously and logs the test data needed to analyze grease-bearing combinations. It realizes several functions such as measuring friction torque, as well as, the self-induced temperature in the bearing under the conditions of an electric motor. The test rig has the ability to apply electric potential to the bearings, apply different radial loads, change speed and is also adaptable to various bearing sizes.

# 6 RECOMMENDATIONS AND FUTURE WORK

This project is scheduled to continue in the following semester in autumn 2018. To finalize this design, the details of Design E must be determined. Additional calculations such as static and dynamic analysis of the system are to be done to ensure reliability and stability at high speeds. The optimal dimensions for the design must be determined, as well as a final bill of materials. This will allow the team to progress into the purchasing and manufacturing phase. During manufacturing, the shaft has to be balanced properly to eliminate large centrifugal forces. Assembly and testing of the device are also required before the project is fully completed.

**Table 10. Plan for Fall 2018 Semester**

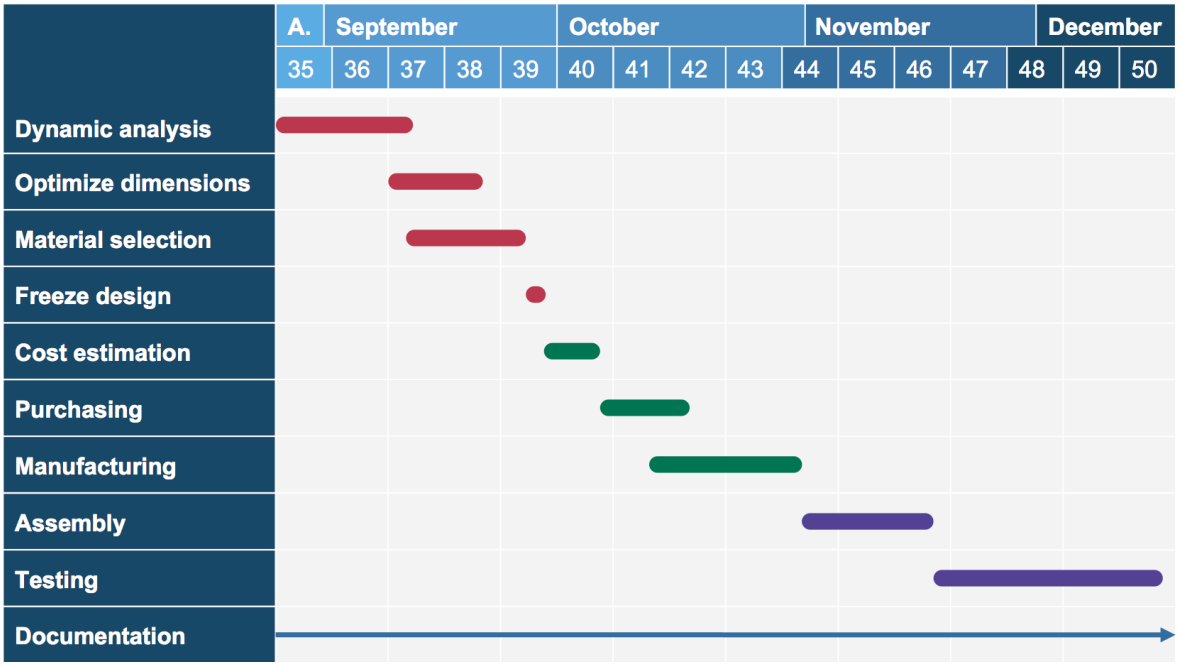

# 7 REFERENCES

American Roller Bearing Company. (2017). *Friction and Frequency Factors*. Retrieved from (Source: https://www.amroll.com/friction-frequency-factors.html)

Axel Christiernsson. (2018). *Axel Ch*. Retrieved from http://www.axelch.com/our-concept/customised-labe

Beeline Engineering Group. (2018). Retrieved from Gates Eurogrip Flexible Couplings: https://industrialbeltdrives.com/quote/flexible-couplings/gates-eurogrip-couplings/

Gralde, M. (2014). *Realisation and evaluation of a start-stop journal bearing test-rig.* Stockholm: KTH.

Jelaska, D. (2012). *Gear and gear drives.*

Mechanical, ME. (2018). *Belts - Types, Advantages and Disadvantages*. Retrieved from https://me-mechanicalengineering.com/belt-drives/

Noria Corporation. (n.d.). *Machinery Lubrication*. Retrieved from http://www.machinerylubrication.com/Read/30210/high-speed-grease

# 8 APPENDIX

## 8.1 Appendix A: MATLAB Code for Angular Twist

```
function
[xx,Delta,Slope,sx,tau,Mb,TT,R,Ktb,Ktt]=SteppedShaft2D(xR,xF,F,xM,M,xT,T,E,xD,D,D
i,xSC,SC,N,PLOT)
% Calculates stresses and deformations in stepped shafts
% xx=x-coordinates
%



%Angle of twist calculations for segment

%Goal: optimize the length, outer diameter, and inner diameter
%Constraint: must not have deflection greater than 0.25mm

%Estimation of values/ranges
mintorque=0.05;%Nm
lengthrange=[0.001:0.001:.5];%m
ID=.015;%m

%Inner diameter for optical torque sensors by Zettlex
miniODrange=[.005, .006, .00635, .008, .010, .012, .0127];%m
midiODrange=[.025, .040, .050, .075, .100, .125, .150, .175, .200, .250];%m
OD= midiODrange(3);

%Given by sensor specification
maxdeflection=0.00025;%m
miniresolution=0.00275;%degrees
midiresolution=0.00017;%degrees

%Minimum twist in meters for midi and mini sensors
count=5;
minitwist=((miniresolution*count)/360)*pi*OD;%m
miditwist=((midiresolution*count)/360)*pi*OD;%m

%Material properties
steelG = 80*10^9;%N/m^2
rubberG = 0.002*10^9;%N/m^2

steelJ = (pi/2)*(ID^4);
rubberJ = (pi/2)*((OD^4)-(ID^4));

steeltwist= mintorque*lengthrange/ (steelG*steelJ);
rubbertwist= mintorque*lengthrange/ (rubberG*rubberJ);

totaltwist= steeltwist + rubbertwist;

%Plot the total twist vs the length
figure(4)
plot(lengthrange,steeltwist,lengthrange,rubbertwist,lengthrange,totaltwist)
title('Angular Twist per Shaft Length')
xlabel('Shaft Length')
ylabel('Angle of Twist')
```

```
%The best length for torque sensor segment is the one with the least
%length to get the required angle of twist
if OD<.015
    minL=(minitwist*(((steelG*steelJ)/mintorque)+...
        (rubberG*rubberJ)/mintorque))*10^3;%m
else
    minL=(miditwist*(((steelG*steelJ)/mintorque)+...
        (rubberG*rubberJ)/mintorque))*10^3;%m
end

display(minL);%mm

%Input the step dimensions in mm
Lbegin=0;
L1=30;      %1 Length until first step
L2=30+L1;   %2 Length between support bearings
L3=minL+10+L2; %3 Length where torque sensor is (+10 for width of devices)
L4=12+L3;   %4 Segment for test bearing

D1=35;      %1 Diameter until first step
D2=60;      %2 Diameter between support bearings
D3=ID*10^3; %3 Diameter where torque sensor is
D4=40;      %4 ID of test bearing 6208
Dend=0;


%Start of Stefan's stepped shaft code

if nargin==0
            xR=[(L1-.9) (L2+.9)]*1e-3;
            xF=[2 (L4-2)]*1e-3;
             F=-[200 1000];
            xM=[];
            M=[];
            xT=[0 15 95 165]*1e-3;
            T=[100 -100 100 -100]*1e-3;
            xSC=[];
            SC=[];
            xD=[Lbegin L1 L1 L2 L2 L3 L4]*1e-3;%Step lengths
            D=[D1 D1 D2 D2 D3 D4 Dend]*1e-3;%Step diameters
            E=500000e6;

%The following two rows shoud always be evaluated when nargin==0
    PLOT=1;
    N=1000; %Number of calculation points
end

if exist('Di')~=1 Di=zeros(size(D)); end
if numel(N)==0 N=100; end
if numel(PLOT)==0 PLOT=0; end

NF=size(F,1);NM=size(M,1);
if size(F,1)==2
    if size(M,1)==0 xM=0; M=[0;0]; end;
    if size(M,1)==1 M=[M;zeros(size(M))]; end;
end
if size(M,1)==2
    if size(F,1)==0 xF=0; F=[0;0]; end;
    if size(F,1)==1 F=[F;zeros(size(F))]; end;
end
if size(F,1)==0 xF=0;F=0; end
if size(M,1)==0 xM=0;M=0; end

s='yz';
for np=1:size(F,1)
```

```
    %Calculate bearing forces
    Rtmp=-(sum(F(np,:).*(xF-xR(1)))+sum(M(np,:)))/diff(xR);
    R(np,1:2)=[-Rtmp-sum(F(np,:)) Rtmp];
    %disp(['RA' s(np) '=' num2str(R(np,1),4) ' N'])
    %disp(['RB' s(np) '=' num2str(R(np,2),4) ' N'])

    %Calculate bending moments
    xP=[xF xR];
    P=[F(np,:) R(np,:)];
    [xP,I]=sort(xP);
    P=P(I);

    xP=[xP;xP+1e-14];xP=xP(:)'; %Make xP-vector with two values for each node
    P=[zeros(size(P));P];P=P(:)'; %First double value zero next P
    xMm=[xM;xM+1e-14];xMm=xMm(:)'; %Make xMm-vector with two values for each node
    Mm=[zeros(size(M(np,:)));M(np,:)];Mm=Mm(:)'; %First double value zero next M
    XD=[xD-1e-14;xD];XD=XD(:)'; %Make xP-vector with two values for each node
    Dd=[0 D(1:end-1);D];Dd=Dd(:)'; %First double value zero next P

    X=[xP xMm XD]; %Nodes along the shaft where something changes
    [x,I]=sort([xP-eps xMm+eps XD]); %Make sure equal xP and xM are separated
correctly
    %X=[xP xMm]; %Nodes along the shaft where something changes
    %[x,I]=sort([xP-eps xMm+eps]); %Make sure equal xP and xM are separated
correctly
    PP=zeros(size(x));MM=PP;DD=PP;
    PP(I<=numel(P))=P; %New load vector with reaction forces included
    MM(I>numel(P)&I<=numel(P)+numel(Mm))=Mm; %Moments applied in node vector

    DD=zeros(size(x));DDi=DD;
    for i=1:numel(D)-1
        v=find(x>=xD(i)&x<xD(i+1));
        DD(v)=D(i);DDi(v)=Di(i);
    end

    S=cumsum(-PP); % Shear forces
    MS=[0 cumsum(S(1:end-1).*diff(x))]; %Bending moment from shear forces only
    MB=cumsum(MM)+MS; %Total bending moment

    v=find(DD~=0);
    MoEI=zeros(size(x));
    MoEI(v)=-MB(v)./(pi*DD(v).^4/64)/E;

    % Calculate slope and deflection
    xx=min(x):(max(x)-min(x))/N:max(x);
    Slope=zeros(size(xx));Delta=Slope;
    A=0;
    v=find(diff(x)>1e-12);
    for i=1:numel(v)
        k=(MoEI(v(i)+1)-MoEI(v(i)))/(x(v(i)+1)-x(v(i)));
        m=MoEI(v(i))-k*x(v(i));
        w=find(xx>=x(v(i))&xx<x(v(i)+1)+1e-13);
        Slope(w)=sum(A)+k/2*(xx(w).^2-x(v(i))^2)+m*(xx(w)-x(v(i)));
        A=[A (MoEI(v(i)+1)+MoEI(v(i)))/2*(x(v(i)+1)-x(v(i)))];
    end
    Slope=Slope-interp1(xx,Slope,(max(xx)-min(xx))/2);
    Delta=cumsum(Slope)*(xx(2)-xx(1));
    [~,i]=min(abs(xx-xR(1)));
    [~,j]=min(abs(xx-xR(2)));
    a=atan((Delta(j)-Delta(i))/(xx(j)-xx(i)));
    Slope=Slope-a;
    Delta=cumsum(Slope)*(xx(2)-xx(1));
    Delta=Delta-interp1(xx,Delta,xR(1));

    if np==1 && size(F,1)==2
```

```
        S_tmp=S;
        MB_tmp=MB;
        MoEI_tmp=MoEI;
        Delta_tmp=Delta;
        Slope_tmp=Slope;
    end
    [xs,I]=sort(x);
    v=find(diff(xs)<=0);
    xs(v+1)=[];
    I(v+1)=[];
    if np==2
        S=[S_tmp;S];
        Ttot=sqrt(interp1(xs,S(1,I),xx).^2+interp1(xs,S(2,I),xx).^2);
        MB=[MB_tmp;MB];
        MBtot=sqrt(interp1(xs,MB(1,I),xx).^2+interp1(xs,MB(2,I),xx).^2);
        MoEI=[MoEI_tmp;MoEI];
        MoEItot=sqrt(interp1(xs,MoEI(1,I),xx).^2+interp1(xs,MoEI(2,I),xx).^2);
        Delta=[Delta_tmp;Delta];
        Deltatot=sqrt(Delta(1,:).^2+Delta(2,:).^2);
        Slope=[Slope_tmp;Slope];
        Slopetot=sqrt(Slope(1,:).^2+Slope(2,:).^2);
    end
end

%Calculate stresses and shear stresses from bending and torsion
if sum(T)~=0 error('Torque equilibrium not fulfilled'); end
TT=zeros(size(xx));
for i=1:numel(T)-1 v=find(xx>=xT(i) & xx<xT(i+1)); TT(v)=sum(T(1:i)); end
if size(F,1)==1 Mb=interp1(xs,MB(I),xx); else Mb=MBtot; end
dd=interp1(xs,DD(I),xx);
ddi=interp1(xs,DDi(I),xx);
Ktb=ones(size(xx));Ktt=Ktb;
for i=1:size(SC,2)
    [~,j]=min(abs(xx-xSC(i)));
    Ktb(j)=SC(1,i);
    Ktt(j)=SC(2,i);
end
sx=32/pi*Mb.*dd./(dd.^4-ddi.^4).*Ktb;
tau=16/pi*TT.*dd./(dd.^4-ddi.^4).*Ktt;
se=sqrt(sx.^2+3*tau.^2);

xx=xx';



%% Plotting
if PLOT
    figure(1);clf
    for i=1:numel(D)-1
        fill([0 1 1 0]*(xD(i+1)-xD(i))+xD(i),[-1 -1 1 1]/2*D(i),[1 1 1]*0.8);hold
on
        fill([0 1 1 0]*(xD(i+1)-xD(i))+xD(i),[-1 -1 1 1]/2*Di(i),[1 1 1]*1);
    end
    plot(x([1 end]),[0 0],'k--')
    axis equal
    YL=diff(get(gca,'Ylim'));
    maxF=max(abs([F(1,:) R(1,:)]));
    ud='^v';TN=40;
    if NF>0 %Only plot forces if original number of forces > 0
        for i=1:numel(xF)
            h=plot(xF(i)*[1 1],F(1,i)/maxF*YL/2.5*[0
1],'b',xF(i),F(1,i)/maxF*YL/2.5,['b' ud(1+(F(1,i)<0))]);
            if size(F,1)==1

h=text(xF(i),F(1,i)/maxF*YL/2.5+sign(F(1,i))*YL/TN,[num2str(F(1,i),4) ' N']);
```

```
            else
                h=text(xF(i),F(1,i)/maxF*YL/2.5+sign(F(1,i))*YL/TN,['y:'
num2str(F(1,i),4) ', z:' num2str(F(2,i),4) ' N']);
            end

set(h,'VerticalAlignment','Middle','HorizontalAlignment','Center','FontSize',8,'C
olor','b','BackGroundColor','w')
        end
    end
    for i=1:numel(xR)
        h=plot(xR(1,i)*[1 1],R(1,i)/maxF*YL/2.5*[0
1],'r',xR(i),R(1,i)/maxF*YL/2.5,['r' ud(1+(R(1,i)<0))]);
        if size(F,1)==1
            h=text(xR(i),R(1,i)/maxF*YL/2.5+sign(R(1,i))*YL/TN,[num2str(R(i),4) '
N']);
        else
            h=text(xR(i),R(1,i)/maxF*YL/2.5+sign(R(1,i))*YL/TN,['y:'
num2str(R(1,i),4) ', z:' num2str(R(2,i),4) ' N']);
        end

set(h,'VerticalAlignment','Middle','HorizontalAlignment','Center','FontSize',8,'C
olor','r','BackGroundColor','w')
    end
    YL=diff(get(gca,'Ylim'));XL=diff(get(gca,'Xlim'));
    fill([-1 0 1]*XL/40*0.8+xR(1),[-1 0 -1]*XL/40,'b');
    fill([-1 0 1]*XL/40*0.8+xR(2),[-1 0 -1]*XL/40,'b');
    if NM>0 %Only plot moments if original number of moments > 0
        for i=1:numel(xM)
            if M(1,i)<0
                fi=(180:-10:-90);
                h=plot(xM(i)+YL/15*cosd(fi),YL/15*sind(fi),'m');
                h=plot(xM(i)+YL/15*cosd(fi(end)),YL/15*sind(fi(end)),'m<');
            else
                fi=(0:10:270);
                h=plot(xM(i)+YL/15*cosd(fi),YL/15*sind(fi),'m');
                h=plot(xM(i)+YL/15*cosd(fi(end)),YL/15*sind(fi(end)),'m>');
            end
            if size(M,1)==1
                h=text(xM(i),YL/15+YL/TN,[num2str(M(1,i),4) ' Nm']);
            else
                h=text(xM(i),YL/15+YL/TN,['y:' num2str(M(1,i),4) ', z:'
num2str(M(2,i),4) ' Nm']);
            end

set(h,'VerticalAlignment','Middle','HorizontalAlignment','Center','FontSize',8,'C
olor','m','BackGroundColor','w')
        end
    end
    h=plot(x,DD/2,x,-DD/2);set(h,'Color',[1 1 1]*0);
    hold off
    xlabel('x [m]');ylabel('y [m]');title('Shaft, forces and torques')
    axis equal
    XLIM=get(gca,'Xlim');

    figure(2)
    subplot(4,1,1)
    h=plot(x,S');set(h,'LineWidth',1+(size(F,1)==1));
    if size(F,1)==2
        hold on;
        h=plot(xx,Ttot,'k');set(h,'LineWidth',2);
        legend('T_x_y','T_x_z','T_t_o_t','Location','Best');
        hold off;
    end
    xlabel('x [m]');ylabel('T [N]');title('Shear force diagram')
    set(gca,'Xlim',XLIM);grid
```

```
    subplot(4,1,2)
    h=plot(x,MB');set(h,'LineWidth',1+(size(F,1)==1));
    if size(F,1)==2
        hold on;
        h=plot(xx,MBtot,'k');set(h,'LineWidth',2);
        legend('M_x_y','M_x_z','M_t_o_t','Location','Best');
        hold off;
    end
    xlabel('x [m]');ylabel('M [Nm]');title('Bending moment diagram')
    set(gca,'Xlim',XLIM);grid

    subplot(4,1,3)
    h=plot(x,MoEI');set(h,'LineWidth',1+(size(F,1)==1));
    if size(F,1)==2
        hold on;
        h=plot(xx,MoEItot,'k');set(h,'LineWidth',2);
        legend('M/EI_x_y','M/EI_x_z','M/EI_t_o_t','Location','Best');
        hold off;
    end
    xlabel('x [m]');ylabel('M/EI [m^-^1]');title('M/EI-diagram')
    set(gca,'Xlim',XLIM);grid

    subplot(4,1,4)
    h=plot(xx,TT');set(h,'LineWidth',2);
    if size(F,1)==2 set(h,'Color','k'); end
    xlabel('x [m]');ylabel('T [Nm]');title('Torque diagram')
    set(gca,'Xlim',XLIM);grid

    figure(3);clf
    subplot(3,1,1)
    h=plot(xx,[sx' tau' se']*1e-6);set(h(3),'LineWidth',2)
    set(gca,'Xlim',XLIM);grid
    xlabel('x [m]');ylabel('Stresses [MPa]');
    legend('s_x','tau','s_v_M')

    subplot(3,1,2)
    h=plot(xx,Slope'*180/pi*60);set(h,'LineWidth',1+(size(F,1)==1))
    hold on
    if size(F,1)==2
        h=plot(xx,Slopetot*180/pi*60,'k');set(h,'LineWidth',2);
        legend('S_x_y','S_x_z','S_t_o_t','Location','Best');
    end
    YLIM=get(gca,'Ylim');
    plot([1 1]*xR(1),YLIM,'k--',[1 1]*xR(2),YLIM,'k--');
    hold off
    set(gca,'Xlim',XLIM);grid
    xlabel('x [m]');ylabel('Relative slope [Minutes of arc]');
    [~,i]=min(abs(xx-xR(1)));
    [~,j]=min(abs(xx-xR(2)));
    if size(F,1)==1 SR=[Slope(i) Slope(j)]*180/pi*60; else SR=[Slopetot(i)
Slopetot(j)]*180/pi*60; end
    title(['Relative slope (at supports: ' num2str(SR(1),3) ' and '
num2str(SR(2),3) ' min of arc)'])

    subplot(3,1,3)
    % xbok=[0 107 152 276 400 530 646 680 716 1060]*1e-3;
    % dbok=[3.8 0 -1.6 -6.125 -10.86 -11.93 -3.79 0 4.13 43.6];
    % plot(xx,delta*1e6,xbok,dbok,'o',[1 1]*xR(1),dmm,'c--',[1 1]*xR(2),dmm,'c--
')
    h=plot(xx,Delta'*1e6);set(h,'LineWidth',1+(size(F,1)==1))
    hold on;
    if size(F,1)==2
        h=plot(xx,Deltatot*1e6,'k');set(h,'LineWidth',2);
        legend('D_x_y','D_x_z','D_t_o_t','Location','Best');
```

```
        STR=num2str(max(abs(Deltatot))*1e3,3);
    else
        STR=num2str(max(abs(Delta))*1e3,3);
    end
    YLIM=get(gca,'Ylim');
    plot([1 1]*xR(1),YLIM,'k--',[1 1]*xR(2),YLIM,'k--');
    xlabel('x [m]');ylabel('Delta [?m]')
    title(['Deflection (max ' STR ' mm)'])
    grid
    set(gca,'Xlim',XLIM);
    hold off
    %keyboard
end
if nargout==0 clear xx; end
```

## 8.2 Appendix B: Original Stepped Shaft MATLAB by Stefan Bjorklund

```
function
[xx,Delta,Slope,sx,tau,Mb,TT,R,Ktb,Ktt]=SteppedShaft2D(xR,xF,F,xM,M,xT,T,E,xD,D,D
i,xSC,SC,N,PLOT)
% Calculates stresses and deformations in stepped shafts
% xx=x-coordinates
%

if nargin==0
            xR=[53 157]*1e-3;
            xF=[100 120]*1e-3;
             F=-[200 600 ];
            xM=[];
            M=[];
            xT=[0 15 95 165]*1e-3;
            T=[100 -100 100 -100]*1e-3;
            xSC=[];
            SC=[];
            xD=[0 30 60 80 110 150 180]*1e-3;
            D=[15 20 30 20 15 12 0]*1e-3;
            E=500000e6;

    %         xR=[30 60]*1e-3;
    %         xF=[20 50 70]*1e-3;
    %         F=-[400 200 300];
    %         xM=[10 40 50 80]*1e-3;
    %         M=[4 -3 2 -1];
    %         xD=[0 25 35 55 65 75 90]*1e-3;
    %         D=[10 12 15 12 10 8 0]*1e-3;
    %         E=207000e6;

    %Sample problem 5.3 p 187 Juvinall and Marshek
%     xR=[0 500]*1e-3;
%     xF=[100 300]*1e-3;
%     F=-[1500 2500];
%     xM=[]*1e-3;
%     M=[];
%     xT=[0 300]*1e-3;
%     T=[1000 -1000]/4;
%     xD=[0 10 150 250 490 500]*1e-3;
%     D=[30 40 60 50 40 0]*1e-3;
%     Di=ones(size(D))*min(D(D>0))*0.5;
%     E=207000e6;

    %   Exam MF2010 2016a nr 1 Q2
    %     xR=[0 2800]*1e-3;
    %     xF=[800 2000]*1e-3;
    %     F=-[1.2*4970 0
    %         0 1.2*4970];
    %     xM=[]*1e-3;
    %     M=[];
    %     xD=[0 2800]*1e-3;
    %     D=[103.75 0]*1e-3;
    %     E=206000e6;

    %   Exam MF2010 20150318 Q2
    %     xR=[0 750]*1e-3;
    %     xF=[300 550]*1e-3;
    %     F=[0 58+50/sqrt(2)
```

```
%         -145 50/sqrt(2)];
%     xM=[]*1e-3;
%     M=[];
%     xD=[0 750]*1e-3;
%     D=[10 0]*1e-3;
%     E=206000e6;

%Exam MF2010 20150318 Q2
%         xR=[0 1200]*1e-3;
%         xF=[200 1000]*1e-3;
%         F=[900 -900]
%         xM=[]*1e-3;
%         M=[];
%         xD=[0 1200]*1e-3;
%         D=[26 0]*1e-3;
%         E=206000e6;

%         xR=[0 750]*1e-3;
%         xF=[300 550]*1e-3;
%         F=[0 58+50/sqrt(2)
%             -145 50/sqrt(2)];
%         xM=[]*1e-3;
%         M=[];
%         xD=[0 100 400 600 650 750]*1e-3;
%         D=[10 15 20 15 10 0]*1e-3;
%         E=206000e6;

% Mott example p 548
%     xR=[254 889]*1e-3;
%     xF=[0 635]*1e-3;
%     F=[-9342 -18685
%         3400 -6800];
%     xM=[]*1e-3;
%     M=[];
%     xT=[0 635]*1e-3;
%     T=[2389 -2389];
%     xD=[0 27 234 274 605 869 889]*1e-3;
%     D=[74 76.3 90.17 97 93.5 80 0]*1e-3;
%     Di=ones(size(D))*50e-3;
%     E=207000e6;

% ISO 6336-1 example p 96
%     xR=[0 150]*1e-3;
%     xF=[50 103]*1e-3;
%     F=[-13500 9000];
%     xM=[]*1e-3;
%     M=[];
%     xT=[]*1e-3;
%     T=[];
%     xD=[0 22 78 128 150]*1e-3;
%     D=[35 50 44 38 0]*1e-3;
%     Di=ones(size(D))*0e-3;
%     xSC=[];
%     SC=[];
%     E=207000e6;

%Used for testing indeterminate shaft calculation
%     F4=1.4912e+04;
%     F21=0;
%     F22=F4*100.7794/120.9353;
%     a=[18   55.4213   90.0926   68.9213   44.7092   31.2092   18]*1e-3;
%     L=sum(a(2:6));
%     b=sum(a(5:6));
%     aa=[sum(a(4:6)) sum(a(3:6)) L];
%     Q=(aa-b)/b*L^3-aa/b*(L-b)^3+(L-aa).^3-b*(aa-b)*L;
```

```
%     Rc=1/Q(3)*(F21*Q(1)+F22*Q(2)-F4*a(6)*a(5)*(1+a(6)/b)*sum(a(2:4)));
%
%     xR=[sum(a(2:4)) sum(a(2:6))];
%     xF=[0 a(2) sum(a(2:3)) sum(a(2:5))];
%     F=[Rc -F22 -F21 -F4];
%     xM=[]*1e-3;
%     M=[];
%     xT=[]*1e-3;
%     T=[]/4;
%     xD=[0 sum(a(2:6))];
%     D=[30 0]*1e-3;
%     Di=ones(size(D))*min(D(D>0))*0.5;
%     E=207000e6;
%
    %   Norton p 954 Overhung beam with concentrated loading
%     L=150e-3;
%     a=130e-3;
%     b=25e-3;
%         xR=[0 b];
%         xF=[a];
%         F=-10000;
%         xM=[];
%         M=[];
%         xT=[];
%         T=[]/4;
%         xD=[0 L];
%         D=[20 0]*1e-3;
%         E=206000e6;
%     xN=(0:L/1000:L);
%     I=pi*D(1)^4/64;
%     ThNorton=-F/2/E/I*((b-a)/b*xN.^2+a/b*(xN-b).^2.*(xN>b)-(xN-
a).^2.*(xN>a)+b/3*(a-b));
%     DaNorton=-F/6/E/I*((b-a)/b*xN.^3+a/b*(xN-b).^3.*(xN>b)-(xN-
a).^3.*(xN>a)+b*(a-b)*xN);

% MF2010 reexam Q2 170608
%     xR=[0 510]*1e-3;
%     xF=[230 810]*1e-3;
%     F=[3312 -2070];
%     xM=[]*1e-3;
%     M=[];
%     xD=[0 810]*1e-3;
%     xT=[230 810]*1e-3;
%     T=[306 -306];
%     D=[50 0]*1e-3;
%     xSC=[];
%     SC=[];
%     E=206000e6;

% MF2005 reexam Q16 171220
%     xR=[0 600]*1e-3;
%     xF=[150 300 450]*1e-3;
%     F=[-2000 0 -2000
%         0 -2667 0];
%     xM=[]*1e-3;
%     M=[];
%     xT=[150 300 450]*1e-3;
%     T=[-80 160 -80];
%     xD=[0 600]*1e-3;
%     D=[40 0]*1e-3;
%     Di=ones(size(D))*0e-3;
%     xSC=[];
%     SC=[];
%     E=210000e6;
```

```
% MF2010 Exam Q2b 140319
%     xR=[0 500]*1e-3;
%     xF=[250 650]*1e-3;
%     F=[0 -500
%        -950 0];
%     xM=[]*1e-3;
%     M=[];
%     xT=[250 650]*1e-3;
%     T=[-1 1]*150*0.05;
%     xD=[0 650]*1e-3;

%     D=[17.2 0]*1e-3;
%     Di=ones(size(D))*0e-3;
%     xSC=[];
%     SC=[];
%     E=206000e6;

%The following two rows shoud always be evaluated when nargin==0
    PLOT=1;
    N=1000; %Number of calculation points
end

if exist('Di')~=1 Di=zeros(size(D)); end
if numel(N)==0 N=100; end
if numel(PLOT)==0 PLOT=0; end

NF=size(F,1);NM=size(M,1);
if size(F,1)==2
    if size(M,1)==0 xM=0; M=[0;0]; end;
    if size(M,1)==1 M=[M;zeros(size(M))]; end;
end
if size(M,1)==2
    if size(F,1)==0 xF=0; F=[0;0]; end;
    if size(F,1)==1 F=[F;zeros(size(F))]; end;
end
if size(F,1)==0 xF=0;F=0; end
if size(M,1)==0 xM=0;M=0; end

s='yz';
for np=1:size(F,1)
    %Calculate bearing forces
    Rtmp=-(sum(F(np,:).*(xF-xR(1)))+sum(M(np,:)))/diff(xR);
    R(np,1:2)=[-Rtmp-sum(F(np,:)) Rtmp];
    %disp(['RA' s(np) '=' num2str(R(np,1),4) ' N'])
    %disp(['RB' s(np) '=' num2str(R(np,2),4) ' N'])

    %Calculate bending moments
    xP=[xF xR];
    P=[F(np,:) R(np,:)];
    [xP,I]=sort(xP);
    P=P(I);

    xP=[xP;xP+1e-14];xP=xP(:)'; %Make xP-vector with two values for each node
    P=[zeros(size(P));P];P=P(:)'; %First double value zero next P
    xMm=[xM;xM+1e-14];xMm=xMm(:)'; %Make xMm-vector with two values for each node
    Mm=[zeros(size(M(np,:)));M(np,:)];Mm=Mm(:)'; %First double value zero next M
    XD=[xD-1e-14;xD];XD=XD(:)'; %Make xP-vector with two values for each node
    Dd=[0 D(1:end-1);D];Dd=Dd(:)'; %First double value zero next P

    X=[xP xMm XD]; %Nodes along the shaft where something changes
    [x,I]=sort([xP-eps xMm+eps XD]); %Make sure equal xP and xM are separated
correctly
    %X=[xP xMm]; %Nodes along the shaft where something changes
    %[x,I]=sort([xP-eps xMm+eps]); %Make sure equal xP and xM are separated
```

```
correctly
    PP=zeros(size(x));MM=PP;DD=PP;
    PP(I<=numel(P))=P; %New load vector with reaction forces included
    MM(I>numel(P)&I<=numel(P)+numel(Mm))=Mm; %Moments applied in node vector

    DD=zeros(size(x));DDi=DD;
    for i=1:numel(D)-1
        v=find(x>=xD(i)&x<xD(i+1));
        DD(v)=D(i);DDi(v)=Di(i);
    end

    S=cumsum(-PP); % Shear forces
    MS=[0 cumsum(S(1:end-1).*diff(x))]; %Bending moment from shear forces only
    MB=cumsum(MM)+MS; %Total bending moment

    v=find(DD~=0);
    MoEI=zeros(size(x));
    MoEI(v)=-MB(v)./(pi*DD(v).^4/64)/E;

    % Calculate slope and deflection
    xx=min(x):(max(x)-min(x))/N:max(x);
    Slope=zeros(size(xx));Delta=Slope;
    A=0;
    v=find(diff(x)>1e-12);
    for i=1:numel(v)
        k=(MoEI(v(i)+1)-MoEI(v(i)))/(x(v(i)+1)-x(v(i)));
        m=MoEI(v(i))-k*x(v(i));
        w=find(xx>=x(v(i))&xx<x(v(i)+1)+1e-13);
        Slope(w)=sum(A)+k/2*(xx(w).^2-x(v(i))^2)+m*(xx(w)-x(v(i)));
        A=[A (MoEI(v(i)+1)+MoEI(v(i)))/2*(x(v(i)+1)-x(v(i)))];
    end
    Slope=Slope-interp1(xx,Slope,(max(xx)-min(xx))/2);
    Delta=cumsum(Slope)*(xx(2)-xx(1));
    [~,i]=min(abs(xx-xR(1)));
    [~,j]=min(abs(xx-xR(2)));
    a=atan((Delta(j)-Delta(i))/(xx(j)-xx(i)));
    Slope=Slope-a;
    Delta=cumsum(Slope)*(xx(2)-xx(1));
    Delta=Delta-interp1(xx,Delta,xR(1));

    if np==1 && size(F,1)==2
        S_tmp=S;
        MB_tmp=MB;
        MoEI_tmp=MoEI;
        Delta_tmp=Delta;
        Slope_tmp=Slope;
    end
    [xs,I]=sort(x);
    v=find(diff(xs)<=0);
    xs(v+1)=[];
    I(v+1)=[];
    if np==2
        S=[S_tmp;S];
        Ttot=sqrt(interp1(xs,S(1,I),xx).^2+interp1(xs,S(2,I),xx).^2);
        MB=[MB_tmp;MB];
        MBtot=sqrt(interp1(xs,MB(1,I),xx).^2+interp1(xs,MB(2,I),xx).^2);
        MoEI=[MoEI_tmp;MoEI];
        MoEItot=sqrt(interp1(xs,MoEI(1,I),xx).^2+interp1(xs,MoEI(2,I),xx).^2);
        Delta=[Delta_tmp;Delta];
        Deltatot=sqrt(Delta(1,:).^2+Delta(2,:).^2);
        Slope=[Slope_tmp;Slope];
        Slopetot=sqrt(Slope(1,:).^2+Slope(2,:).^2);
    end
end
```

```
%Calculate stresses and shear stresses from bending and torsion
if sum(T)~=0 error('Torque equilibrium not fulfilled'); end
TT=zeros(size(xx));
for i=1:numel(T)-1 v=find(xx>=xT(i) & xx<xT(i+1)); TT(v)=sum(T(1:i)); end
if size(F,1)==1 Mb=interp1(xs,MB(I),xx); else Mb=MBtot; end
dd=interp1(xs,DD(I),xx);
ddi=interp1(xs,DDi(I),xx);
Ktb=ones(size(xx));Ktt=Ktb;
for i=1:size(SC,2)
    [~,j]=min(abs(xx-xSC(i)));
    Ktb(j)=SC(1,i);
    Ktt(j)=SC(2,i);
end
sx=32/pi*Mb.*dd./(dd.^4-ddi.^4).*Ktb;
tau=16/pi*TT.*dd./(dd.^4-ddi.^4).*Ktt;
se=sqrt(sx.^2+3*tau.^2);

xx=xx';

%% Plotting
if PLOT
    figure(1);clf
    for i=1:numel(D)-1
        fill([0 1 1 0]*(xD(i+1)-xD(i))+xD(i),[-1 -1 1 1]/2*D(i),[1 1 1]*0.8);hold
on
        fill([0 1 1 0]*(xD(i+1)-xD(i))+xD(i),[-1 -1 1 1]/2*Di(i),[1 1 1]*1);
    end
    plot(x([1 end]),[0 0],'k--')
    axis equal
    YL=diff(get(gca,'Ylim'));
    maxF=max(abs([F(1,:) R(1,:)]));
    ud='^v';TN=40;
    if NF>0 %Only plot forces if original number of forces > 0
        for i=1:numel(xF)
            h=plot(xF(i)*[1 1],F(1,i)/maxF*YL/2.5*[0
1],'b',xF(i),F(1,i)/maxF*YL/2.5,['b' ud(1+(F(1,i)<0))]);
            if size(F,1)==1

h=text(xF(i),F(1,i)/maxF*YL/2.5+sign(F(1,i))*YL/TN,[num2str(F(1,i),4) ' N']);
            else
                h=text(xF(i),F(1,i)/maxF*YL/2.5+sign(F(1,i))*YL/TN,['y:'
num2str(F(1,i),4) ', z:' num2str(F(2,i),4) ' N']);
            end

set(h,'VerticalAlignment','Middle','HorizontalAlignment','Center','FontSize',8,'C
olor','b','BackGroundColor','w')
        end
    end
    for i=1:numel(xR)
        h=plot(xR(1,i)*[1 1],R(1,i)/maxF*YL/2.5*[0
1],'r',xR(i),R(1,i)/maxF*YL/2.5,['r' ud(1+(R(1,i)<0))]);
        if size(F,1)==1
            h=text(xR(i),R(1,i)/maxF*YL/2.5+sign(R(1,i))*YL/TN,[num2str(R(i),4) '
N']);
        else
            h=text(xR(i),R(1,i)/maxF*YL/2.5+sign(R(1,i))*YL/TN,['y:'
num2str(R(1,i),4) ', z:' num2str(R(2,i),4) ' N']);
        end

set(h,'VerticalAlignment','Middle','HorizontalAlignment','Center','FontSize',8,'C
olor','r','BackGroundColor','w')
    end
    YL=diff(get(gca,'Ylim'));XL=diff(get(gca,'Xlim'));
    fill([-1 0 1]*XL/40*0.8+xR(1),[-1 0 -1]*XL/40,'b');
    fill([-1 0 1]*XL/40*0.8+xR(2),[-1 0 -1]*XL/40,'b');
```

```
    if NM>0 %Only plot moments if original number of moments > 0
        for i=1:numel(xM)
            if M(1,i)<0
                fi=(180:-10:-90);
                h=plot(xM(i)+YL/15*cosd(fi),YL/15*sind(fi),'m');
                h=plot(xM(i)+YL/15*cosd(fi(end)),YL/15*sind(fi(end)),'m<');
            else
                fi=(0:10:270);
                h=plot(xM(i)+YL/15*cosd(fi),YL/15*sind(fi),'m');
                h=plot(xM(i)+YL/15*cosd(fi(end)),YL/15*sind(fi(end)),'m>');
            end
            if size(M,1)==1
                h=text(xM(i),YL/15+YL/TN,[num2str(M(1,i),4) ' Nm']);
            else
                h=text(xM(i),YL/15+YL/TN,['y:' num2str(M(1,i),4) ', z:'
num2str(M(2,i),4) ' Nm']);
            end

set(h,'VerticalAlignment','Middle','HorizontalAlignment','Center','FontSize',8,'C
olor','m','BackGroundColor','w')
        end
    end
    h=plot(x,DD/2,x,-DD/2);set(h,'Color',[1 1 1]*0);
    hold off
    xlabel('x [m]');ylabel('y [m]');title('Shaft, forces and torques')
    axis equal
    XLIM=get(gca,'Xlim');

    figure(2)
    subplot(4,1,1)
    h=plot(x,S');set(h,'LineWidth',1+(size(F,1)==1));
    if size(F,1)==2
        hold on;
        h=plot(xx,Ttot,'k');set(h,'LineWidth',2);
        legend('T_x_y','T_x_z','T_t_o_t','Location','Best');
        hold off;
    end
    xlabel('x [m]');ylabel('T [N]');title('Shear force diagram')
    set(gca,'Xlim',XLIM);grid

    subplot(4,1,2)
    h=plot(x,MB');set(h,'LineWidth',1+(size(F,1)==1));
    if size(F,1)==2
        hold on;
        h=plot(xx,MBtot,'k');set(h,'LineWidth',2);
        legend('M_x_y','M_x_z','M_t_o_t','Location','Best');
        hold off;
    end
    xlabel('x [m]');ylabel('M [Nm]');title('Bending moment diagram')
    set(gca,'Xlim',XLIM);grid

    subplot(4,1,3)
    h=plot(x,MoEI');set(h,'LineWidth',1+(size(F,1)==1));
    if size(F,1)==2
        hold on;
        h=plot(xx,MoEItot,'k');set(h,'LineWidth',2);
        legend('M/EI_x_y','M/EI_x_z','M/EI_t_o_t','Location','Best');
        hold off;
    end
    xlabel('x [m]');ylabel('M/EI [m^-^1]');title('M/EI-diagram')
    set(gca,'Xlim',XLIM);grid

    subplot(4,1,4)
    h=plot(xx,TT');set(h,'LineWidth',2);
    if size(F,1)==2 set(h,'Color','k'); end
```

```
    xlabel('x [m]');ylabel('T [Nm]');title('Torque diagram')
    set(gca,'Xlim',XLIM);grid

    figure(3);clf
    subplot(3,1,1)
    h=plot(xx,[sx' tau' se']*1e-6);set(h(3),'LineWidth',2)
    set(gca,'Xlim',XLIM);grid
    xlabel('x [m]');ylabel('Stresses [MPa]');
    legend('s_x','tau','s_v_M')

    subplot(3,1,2)
    h=plot(xx,Slope'*180/pi*60);set(h,'LineWidth',1+(size(F,1)==1))
    hold on
    if size(F,1)==2
        h=plot(xx,Slopetot*180/pi*60,'k');set(h,'LineWidth',2);
        legend('S_x_y','S_x_z','S_t_o_t','Location','Best');
    end
    YLIM=get(gca,'Ylim');
    plot([1 1]*xR(1),YLIM,'k--',[1 1]*xR(2),YLIM,'k--');
    hold off
    set(gca,'Xlim',XLIM);grid
    xlabel('x [m]');ylabel('Relative slope [Minutes of arc]');
    [~,i]=min(abs(xx-xR(1)));
    [~,j]=min(abs(xx-xR(2)));
    if size(F,1)==1 SR=[Slope(i) Slope(j)]*180/pi*60; else SR=[Slopetot(i)
Slopetot(j)]*180/pi*60; end
    title(['Relative slope (at supports: ' num2str(SR(1),3) ' and '
num2str(SR(2),3) ' min of arc)'])

    subplot(3,1,3)
    % xbok=[0 107 152 276 400 530 646 680 716 1060]*1e-3;
    % dbok=[3.8 0 -1.6 -6.125 -10.86 -11.93 -3.79 0 4.13 43.6];
    % plot(xx,delta*1e6,xbok,dbok,'o',[1 1]*xR(1),dmm,'c--',[1 1]*xR(2),dmm,'c--
')
    h=plot(xx,Delta'*1e6);set(h,'LineWidth',1+(size(F,1)==1))
    hold on;
    if size(F,1)==2
        h=plot(xx,Deltatot*1e6,'k');set(h,'LineWidth',2);
        legend('D_x_y','D_x_z','D_t_o_t','Location','Best');
        STR=num2str(max(abs(Deltatot))*1e3,3);
    else
        STR=num2str(max(abs(Delta))*1e3,3);
    end
    YLIM=get(gca,'Ylim');
    plot([1 1]*xR(1),YLIM,'k--',[1 1]*xR(2),YLIM,'k--');
    xlabel('x [m]');ylabel('Delta [?m]')
    title(['Deflection (max ' STR ' mm)'])
    grid
    set(gca,'Xlim',XLIM);
    hold off
    %keyboard
end
if nargout==0 clear xx; end
```

## 8.3 Appendix C: Design Component Comparison

| 5 Key Designs | Loading System | | | | Torque Measurement | | | Isolation of the Current | |
|---|---|---|---|---|---|---|---|---|---|
| | Nut and Spring | Actuator across 2 Bearings | Floating Actuator System | Motor Pulley Force | Pressure Sensor | Motor Current | Angular Twist (Optical) | Insulative Sleeve | Coupling |
| A Cantilever Concept | | | ✓ | | | | ✓ | ✓ | |
| B Central Loading | | | ✓ | | | | ✓ | ✓ | |
| C Two Test Bearings | | | | ✓ | | ✓ | | ✓ | |
| D Four Test Bearings | | ✓ | | | | ✓ | | | ✓ |
| E Advanced Cantilever | ✓ | | | | ✓ | | | ✓ | |

| 5 Key Designs | Number of Test Bearings | | Applicable to Bearings | | | Apply Speed | | Disassembly | |
|---|---|---|---|---|---|---|---|---|---|
| | One | Multiple | All 620X | Only 6204 to 6206 | Only 6208 | Directly from Motor | Motor and Pulley | Sleeve w/ Bearing from End | Entire Shaft Replaced |
| A Cantilever Concept | ✓ | | ✓ | | | | ✓ | | ✓ |
| B Central Loading | ✓ | | | | ✓ | | ✓ | | ✓ |
| C Two Test Bearings | | ✓ | | ✓ | | | ✓ | | ✓ |
| D Four Test Bearings | | ✓ | | | ✓ | ✓ | | ✓ | |
| E Advanced Cantilever | ✓ | | ✓ | | | | ✓ | ✓ | |